JOURNAL OF BIOMOLECULAR STRUCTURE AND DYNAMICS
https://doi.org/10.1080/07391102.2021.1973563

Discovery of potential SARS-CoV 3CL protease inhibitors from approved antiviral drugs using: virtual screening, molecular docking, pharmacophore mapping evaluation and dynamics simulation

Ismail Daoud[a,b], Fouzia Mesli[b], Nadjib Melkemi[c], Said Ghalem[b] and Toufik Salah[c]

[a]Department of Matter Sciences, University Mohamed Khider, Biskra, Algeria; [b]Faculty of Science, Laboratory of Natural and Bio-Actives Substances, Tlemcen University, Tlemcen, Algeria; [c]Group of Computational and Pharmaceutical Chemistry LMCE Laboratory, University of Biskra, Algeria

Communicated by Ramaswamy H. Sarma

ABSTRACT

The spread of corona-virus disease 2019 (COVID-19) has been faster than any other corona-viruses that have succeeded in crossing the animal-human barrier. This disease, caused by the severe acute respiratory syndrome corona-virus 2 (SARS-CoV-2/2019-nCoV) posing a serious threat to global public health and local economies. There are three responsible for this disease; SARS-CoV-2, SARS-CoV and MERS-CoV. Whereas our goal is to test the affinity for a new class of compounds obtained from a hybridization of Chloroquine, Amodiaquine and Mefloquine with three targets SARS-CoV-2, SARS-CoV and MERS-CoV, in order to find new compounds as new inhibitors against Covid-19. In this work, we first used: the molecular docking/dynamics methods and ADME properties to study interaction and affinity between eight new compounds against three targets involved in the Covid-19. The results of the docking simulations and dynamics revealed that inhibitor of the malaria (Ligand 87) has an affinity to interact with SARS-CoV-2, SARS-CoV and MERS-CoV targets and they can be good inhibitors for treatment of Covid-19. Moreover, they give best affinity compared to the Remdesivir and Chloroquine and other clinical tests. The Pharmacokinetics was justified by means of lipophilicity and high coefficient of skin permeability. The in silico evaluation of ADME and drug-likeness revealed that L87 has higher absorption in the intestines with good bioavailability. However, an additional *in vitro* and/or *in vivo* experimental study should make it possible to verify the theoretical results obtained in silico.

ARTICLE HISTORY
Received 9 February 2021
Accepted 23 August 2021

KEYWORDS
Covid-19; hybridization of Chloroquine; docking/molecular dynamics; ADME

1. Introduction

Corona-virus has appeared the first time in 2012 at the Arabian Peninsula with a fatality rate of 35%. He was known as SARS-CoV and MERS-CoV. Both SARS-CoV and MERS-CoV are zoonotic viruses, and their hosts are bat/civet and dromedary, respectively (Lau et al., 2005; Reusken et al., 2013). In addition, Common symptoms of a person infected with a corona-virus include respiratory symptoms, fever, cough and shortness of breath. This virus has appeared again in China, which it was identified in Wuhan city, in December 2019 and it spread widely in the whole world because this virus is mainly spread between people during close contact, often via small droplets produced during coughing, sneezing, or talking (Bourouiba, 2020). While these droplets are produced when breathing out, they usually fall to the ground or surfaces rather than being infectious over large distances (National Institutes of Health (NIH), 17 March 2020). According to the World Health Organization (WHO), the Centers for Disease Control and Prevention (CDC), and the U.S. Food and Drug Administration (FDA), there are currently no medications or vaccines proven to be effective for the treatment or prevention of the 2019 severe acute respiratory syndrome corona-virus 2 (SARS-CoV-2). CoVs are belonging to the Coronaviridae family of class Nidovirales and also you knowing that they are enveloped viruses with a positive RNA genome. These viruses are divided into four genera (α, β, γ, and δ). The SARS-CoV-2 belongs to the β genus.

In addition, Bosch et al. (2003) found that there are at least four structural proteins in CoVs: Spike (S) protein, the envelope (E) protein, membrane (M) protein, and nucleocapsid (N) protein. Among them, Spike which is considered host attachment and virus–cell membrane fusion during virus infection. Therefore, Spike determines to some extent the host range. Both the human immune system (human cells), and the corona-virus itself are considered the two targets for potential anti-coronavirus therapies, the innate immune system response plays an important role in controlling the replication and infection of corona-virus (Omrani et al., 2014).

The majority of studies for the treatment of corona-viruses are based on the inhibition of replication of the virus by acting on the blocking of the binding of the virus to receptors in human cells or the inhibition of the auto-detection of the

CONTACT Fouzia Mesli meslifouzia2018@gmail.com; Ismail Daoud i.daoud@univ-biskra.dz Faculty of Science, Laboratory of Natural and Bio-Actives Substances, Tlemcen University, Tlemcen, Algeria

Supplemental data for this article can be accessed online at https://doi.org/10.1080/07391102.2021.1973563.

virus. Three methods to develop new drugs have been developed by scientists to fight the corona-virus (Zumla et al., 2016). The first method is to test anti-virals at a wide range 'broad-spectrum' (Chan et al., 2013) by using inhibitors like ribavirin and cyclophilin for the treatment of corona-virus pneumonia, but the major disadvantage of these therapies is that they cannot kill corona-viruses in a targeted manner, and their side effects should not be underestimated. The second method is to screen for molecules that may have a therapeutic effect on corona-virus by using existing molecular databases (de Wilde et al., 2014; Dyall et al., 2014). This method based on high throughput screening and new functions of many drug molecules can be found through this method, for example discovering the anti-HIV drug. The third method aims to develop new targeted drugs from scratch based solely on the genomic information and pathological characteristics of different corona-viruses. Theoretically, the strategy is very effective and the drugs found thanks to these therapies would exhibit better anti-coronavirus effects, but unfortunately the procedure of research of a new drug by this method could cost several years (Omrani et al., 2014).

After the spread of this incurable disease, a number of vaccines and drugs were proved their efficacy and approved in clinical studies (Wang et al., 2020).

Recently, several vaccines were entered into the clinical evaluation (Le et al., 2020). Among them include: (1) mRNA-vaccines: BioNTech/Pfizer (Müller et al., 2021), Moderna (Mahase, 2020), Inovio as DNA-based vaccines (Calina et al., 2020) and CureVac/Bayer (Rosales-Mendoza et al., 2020). (2) Especially for Viral vector vaccines: AstraZeneca (Wise, 2021), Janssen Vaccines (Livingston et al., 2021) and by Gamaleya Research Institute of Epidemiology and Microbiology (Jones & Roy, 2021). (3) For inactivated virus: Sinovac vaccine (Palacios et al., 2020) developed by China Sinovac Biotech Company. (4) Antigen-based vaccine EpiVacCorona that was developed by the Vector Institute (Ryzhikov et al., 2021).

Currently, inhibition of targets SARS-CoV-2, SARS-CoV and MERS-CoV with novel small molecules have been continuously discovered either from natural products or synthetic by using different methods such as: computational and experimental approach (Alamri et al., 2020; Gao et al., 2020; Gautret et al., 2020; Wu et al., 2020) and lots of drugs tested for the treatment of Covid-19 are discovered based on these targets, among which: Chloroquine (Keyaerts et al., 2004; Vincent et al., 2005), Hydroxy Chloroquine (McChesney et al., 1983), Remdesivir (Warren et al., 2016), Arbidol (Panisheva et al., 1988), Favipiravir (Furuta et al., 2005), Ribavirin (Witkowski et al., 1972) and Sofosbuvir (Bullard-Feibelman et al., 2017) are the seven drugs used like Clinical Trials for the treatment of Covid-19 or initially approved by U.S. FDA such as remdesivir (Beigel et al., 2020). In addition, IFN-I with an established role in suppression and treatment of SARS-CoV, MERS-CoV and SARSCoV-2 infections was also suggested (Lee & Shin, 2020). Also, CR3022 monoclonal antibody with binding affinity to the RBD of SARS-CoV-2 S protein was suggested as a therapeutic approach (Lee et al., 2020).

Several previous studies (Mani et al., 2019; Sakurai et al., 2015) have mentioned that many promising drug candidates for various viral infectious diseases like Ebola, ZIKA, dengue, influenza, HIV, HSV, CMV infections and various other infectious diseases have been probably able to be mainly developed to treat other illnesses such as: MERS- and SARS-CoV, Imatinib Approved/anticancer for MERS- and SARS-CoV.

Recently, Luiz et al. (2019) proves that eight new compound derivatives (Chloroquine, Amodiaquine and Mefloquine) stood out as potent inhibitors against malaria (Figure 1).

In this contribution, a combination of three theoretical approaches based on molecular docking, molecular dynamic simulations and ADME Properties were used to explore potential inhibitors among eight compounds against three coronavirus enzymes: SARS-CoV-2, SARS-CoV and MERS-CoV and then compared to Chloroquine, Hydroxychloroquin, Simeprevir, and Remdesivir an antiviral drugs inhibitors of angiotensin converting enzyme 2 (ACE2) (see Figure 1a, supplementary material).

2. Materials and methods

2.1. Targets and compounds preparations

2.1.1. Targets preparations

The X-ray structures of SARS-CoV-2 (PDB ID: 6LU7) in the bound state with PRD_002214, SARS-CoV (PDB ID: 2A5I) in the bound state with AZP and MERS-CoV (PDB ID: 5WKK) 3CLpro in the bound state with AW4 were retrieved from the protein RCSB Database (http://www.rcsb.org/pdb).

In addition, the validations of the model for the enzyme MERS-CoV (PDB ID: 5WKK) 3CLpro is the most important step in homology modeling. SWISS-MODEL, managed by the Swiss Institute of Bioinformatics (Arnold et al., 2006; Guex et al., 2009; Kiefer et al., 2009) used to find out the evolutionary conserved functional residues among MERS-CoV by identification, protein in the Protein Data Bank (PDB) having high sequence similarity (identical and shares similarity) which could be further targeted as probable target for the discovery of drug hits.

In the last, the energy of the protein structures is minimized using the Energy minimization algorithm of MOE tool. These energies of proteins are calculated (in kcal/mol) by MOE using a MMFF94x force field with conjugant gradient method.

Clément and Slenzka (2006) and Didierjean and Tête-Favier (2016) demonstrate that the protein structure with a resolution between 1.5 and 2.5 Å have a good quality for further studies, whereas, the resolution values of: SARS-CoV-2, SARS-CoV and MERS-CoV targets belong to this interval. In addition, we note that R-value of all enzymes belong to the range of typical values according to Kleywegt and Jones (1997).

For simplify structures of these three enzymes, all ions and Co-crystal ligand molecules were deleted from the structures and the PDBs, but the water molecules were kept because Klebe, G (Klebe et al., 2006) shows that the presence of water is sometimes essential to ensure a relay between the compound and the active site and thus create networks of hydrogen bonds. On the other hand Marechal (Marechal, 2007) confirmed that water molecules in the cavities of

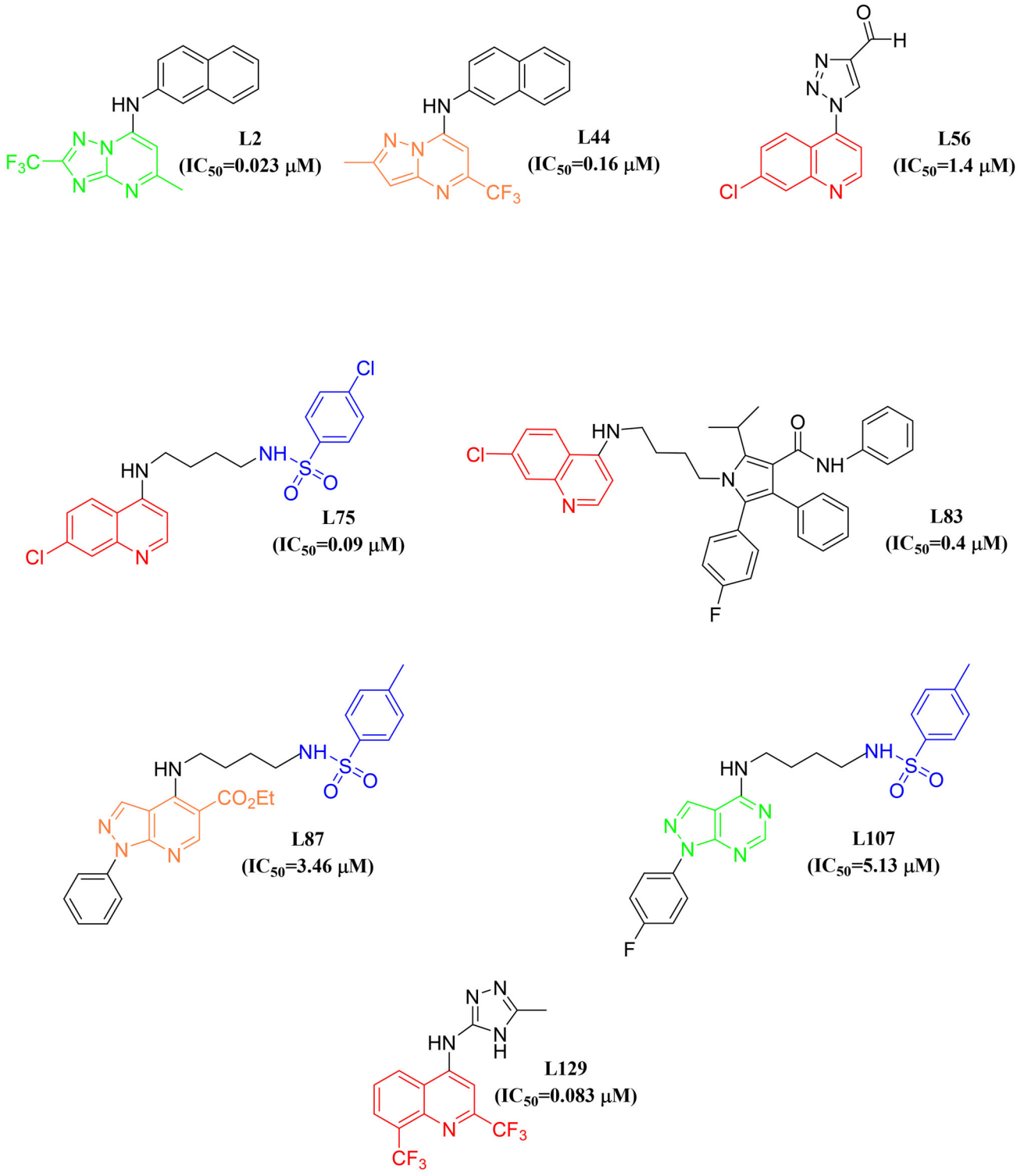

Figure 1. The chemical structures of the compounds tested with their IC_{50} value against malaria.

proteins can sometimes be a fundamental element some algorithms are able to simulate the presence of water molecules in the cavities of proteins.

Validation of molecular docking method is the most important factor for obtains a good and accurate results. Therefore, there are two validations such as (Hevener et al., 2009):

1/Internal validation (searching for <2 Å RMSD).
2/Retrospective Validation (ROC validation).

In our case we used the internal validation and in order to validate the docking method, we re-docked the three co-crystallized ligand (The co-crystallized ligand: of 6LU7 is: PRD_002214 (Peptide), 2A5I is: AZP($C_{32}H_{43}N_5O_9$) and 5WKK is: AW4($C_{22}H_{32}C_lN_3O_8S$) into theirs crystal structures of enzymes using MOE software, and the results obtained of the best poses of three complexes were nearly perfectly superimposed with the native ligand with an RMSD values of **1.195, 1.714** and **1.024 Å** which were lower than 2 Å, the value

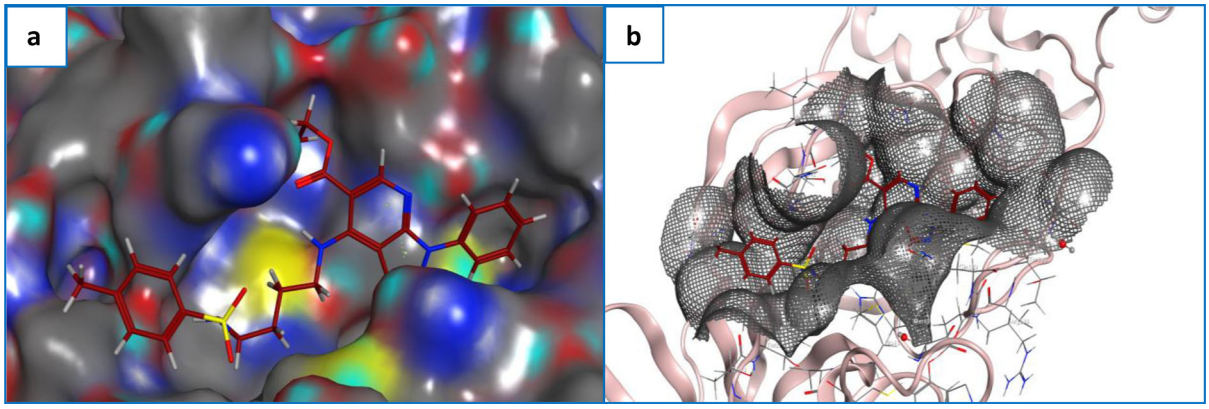

Figure 2. (a) The top scoring compound. (b) A novel inhibitor L-87 identified by molecular docking is shown in the active site.

described in the literature reference, and this values justify the accuracy of this method.

2.1.2. Compounds preparation

The three-dimensional structures of eight compounds tested in malaria (Table 2) were pre-optimized using Hyperchem 8.0.8 software (HyperChem v8, 2009) by means of the Molecular Mechanics using Force Field MM+. After that, the resulted minimized structures were further refined using the semi-empirical method AM1 (Stewart, 2007) with default parameters such as: the Polak-Ribiere conjugate gradient algorithm of 0.01 kcal/(Å mol). The database was created in which all the compounds were converted into their 3 D structures and this database was used as an input for MOE-docking software MOE (Molecular Operating Environment (Moe), 2019) and MVD software (Thomsen & Christensen, 2006) in order to extract the information of all compounds (Table 1).

According to the table above, we note also that the three compounds L83, L87 and L107 have a high value of weight compared to other compounds and also the results obtained show that the these compounds (L83, L87 and L107) have a high value of torsion angle relative to other compounds, this shows that these compounds are more flexible. In addition, it is noted that the growth of the torsion angle depends on the binding number of the molecules.

3. Computational approach

3.1. Molecular docking protocol

Molecular Docking and dynamics simulation was done using MOE software (Molecular Operating Environment (Moe), 2019). MOE-Dock implemented in MOE software was used for identifying different favorable binding (interactions) between compounds and targets which it based on type of molecular mechanics force fields chosen (Halgren, 1996, 1999). For molecular docking calculations, we followed the same steps (same protocol) used in our previous studies (Chenafa et al., 2021; Daoud et al., 2018; Mesli et al., 2021) and the default parameters are: Placement: Triangle Matcher; Rescoring 1: London dG (the scoring function was employed to estimate the lowest free energy of the complex with the best pose of ligand tested). During the docking process the ligand was considered structurally rigid while the target was set as completely flexible.

The results of the top-score docking poses were constructed and the best scoring complexes in the active site were selected for the further MD simulation study (Dal Ben et al., 2013).

3.2. Molecular dynamics (MD) Simulation and pharmacophore mapping protocol

The best pose with lowest score energy obtained by docking procedure was confirmed by (MD) simulations using MOE software witch that uses the Nose Poincare-Andersen (NPA) equations of motion and MMFF94x force field (Bond et al., 1999; Sturgeon & Laird, 2000). Molecular dynamics calculations based on the study of the variation of RMSD as a function of time for complexes (Aryapour et al., 2017; Azam & Jupudi, 2017; Ballu et al., 2018; Hernández-Rodríguez et al., 2016); but the other studies evaluating the variation of potential energy as a function of time (Chaube et al., 2016), in both situations the aim is to show the stability of the complexes. In our case, (MD) simulation employed to analyze the variation of the potential energy as a function of time for all complexes. The minimized system was then heated to desired temperatures under an isothermal ensemble by soft coupling with the Berendsen thermostat (NVT) (Berendsen et al., 1984). In all simulations the van der Waals cut-out distance was set to 8 Å. Molecular dynamic simulations were then carried out in periodic cubic box with minimum distance of 1.0 nm between any atom of the protein and walls of the cubic box. After minimization, heating and equilibration, the production MD phase was carried out at 300 K for 100 ns with a time step of 1 fs using the constant volume and temperature (NVT) ensemble. The Molecular Operating Environment (MOE) software was used for our study because it has proven its performance in several recent studies; we can cite some example of work: Mesli et al. (2019; Nadia et al., 2020). The pharmacophore mapping study of the best ligand L85 was carried out by online server PharmMapper (Parr & Yang, 1980) (http://www.lilab-ecust.cn/pharmmapper/). The pharmacophore mapping experiment was done for the best ligand molecule among the eight selected ligands use for the creation of new drugs (Figure 15). The ligands, downloaded in SDF format from PubChem server, were uploaded and the 'maximum number of conformations' parameter was set at 1000, all possible

targets were kept at the 'select target set' parameter and the 'number of reserved matched targets' parameter was kept 1000. In the advanced options, the cut-off value of fit score was set at 0. All the other parameters were kept at default.

Table 1. Some properties of the studied compounds.

Compounds	Toxic	Rsynth (%)	Weight (g/mol)	TPSA Å^2	Hdon + Hacc	Flexibility
L2	No	100	343.31	39.99	don:1; acc:3	3 out 3
L44	No	84	341.32	39.99	don:1; acc:2	3 out 3
L56	No	100	258.67	60.67	don:0; acc:4	2 out 2
L75	No	100	423.34	59.06	don:1; acc:4	8 out 8
L83	No	100	631.19	58.95	don:2; acc:2	11 out 11
L87	No	100	507.61	115.21	don:2; acc:5	12 out 12
L107	No	100	454.53	101.80	don:2; acc:5	9 out 9
L129	No	100	361.25	66.49	don:2; acc:5	4 out 4

The P450 site of metabolism (SOM) of the three best selected ligand molecules were determined by online tool, RS-WebPredictor 1.0 (http://reccr.chem.rpi.edu/Software/RS-WebPredictor/).

The pharmacophore modelling of the two best ligands was performed using Molecular Operating Environment (MOE) software. Moreover, the P450 SOM prediction, pharmacophore mapping and solubility prediction were carried out to determine and compare the biological activities of the two best ligands molecules.

4. ADME properties

In recent years, the ADME have been developing an important number of parameters for predicting ADME properties

Table 2. S-score (Energy) and interactions between compounds and the active site residues of SARS-CoV-2, SARS-CoV and MERS-CoV targets.

SARS-Cov-2 (PDB ID: 6LU7)							
		Bonds between atoms of compounds and residues of active site					
Compounds	S-score (kcal/mol)	Atom of compound	Involved receptor atoms	Involved receptor residues	Type of interaction bond	Distance (Å)	Energies (kcal/mol)
L2	−6.464	–	–	–	–	–	–
L44	−6.246	–	–	–	–	–	–
L56	−5.597	O-18	NE2	HIS163	H-acceptor	3.42	−0.60
		6-ring	N	GLU166	Pi-H	4.22	−0.90
L75	−6.467	O-45	NE3	HIS163	H-acceptor	3.06	−6.40
L83	−5.392	O-31	SD	MET165	H-donor	4.16	−0.60
L87	**−7.607**	**O-28**	**N**	**GLY143**	**H-acceptor**	**3.02**	**−3.70**
		6-ring	**N**	**THR26**	**pi-H**	**4.41**	**−1.70**
		6-ring	**N**	**GLU166**	**pi-H**	**4.15**	**−0.80**
L107	−6.942	5-ring	N	GLU166	pi-H	4.16	−1.10
L129	**−6.920**	**F-27**	**NE2**	**HIS163**	**H-acceptor**	**2.94**	**−1.20**
		5-ring	**CG**	**GLN189**	**Pi-H**	**4.68**	**−0.80**
SARS-Cov (PDB ID: **2A5I**)							
		Bonds between atoms of compounds and residues of active site					
Compounds	**S-score (kcal/mol)**	**Atom of compound**	**Involved receptor atoms**	**Involved receptor residues**	**Type of interaction bond**	**Distance (Å)**	**Energies (kcal/mol)**
L2	−6.479	6-ring	5-ring	HIS41	pi-pi	3.86	−0.00
L44	−6.109	C-2	OE1	GLN189	H-donor	3.47	−0.80
L56	−5.595	O-18	NE2	HIS163	H-acceptor	3.06	−1.50
		5-ring	O	HOH369	pi-H	3.83	−2.20
		6-ring	5-ring	HIS41	pi-H	3.99	−0.00
L75	−6.887	N-22	O	HOH324	H-donor	3.00	−0.00
L83	−6.836	N-12	SD	MET165	H-donor	4.44	−0.90
L87	**−8.764**	**N-17**	**SD**	**MET49**	**H-donor**	**3.99**	**−1.60**
		N-11	**N**	**GLY143**	**H-acceptor**	**3.63**	**−0.90**
		O-29	**O**	**HOH538**	**H-acceptor**	**3.24**	**−0.90**
		6-ring	**N**	**ALA46**	**Pi-H**	**4.62**	**−0.90**
L107	**−7.309**	**O-23**	**SD**	**MET49**	**H-donor**	**3.87**	**−0.40**
		6-ring	**CB**	**GLU166**	**Pi-H**	**4.10**	**−1.00**
L129	−6.431	–	–	–	–	–	–
MERS-Cov (PDB ID: **5WKK**)							
		Bonds between atoms of compounds and residues of active site					
Compounds	**S-score (kcal/mol)**	**Atom of compound**	**Involved receptor atoms**	**Involved receptor residues**	**Type of interaction bond**	**Distance (Å)**	**Energies (kcal/mol)**
L2	−6.533	N-4	SG	CYS148	H-donor	4.07	−0.30
		N-12	O	HOH517	H-donor	3.19	−2.90
L44	−6.759	–	–	–	–	–	–
L56	−5.870	–	–	–	–	–	–
L75	−6.228	–	–	–	–	–	–
L83	−5.854	O-31	NE2	HIS194	H-acceptor	2.97	−1.60
L87	**−7.074**	**N-17**	**O**	**HOH517**	**H-donor**	**3.11**	**−0.30**
		N-26	**O**	**HOH517**	**H-donor**	**2.99**	**−0.90**
L107	**−6.759**	**N-21**	**OE1**	**GLN192**	**H-donor**	**3.00**	**−4.80**
		O-24	**N**	**GLU169**	**H-acceptor**	**3.37**	**−3.70**
L129	**−6.686**	**N-11**	**O**	**GLN167**	**H-donor**	**3.07**	**−2.80**
		N-14	**SG**	**CYS145**	**H-donor**	**3.26**	**−2.80**

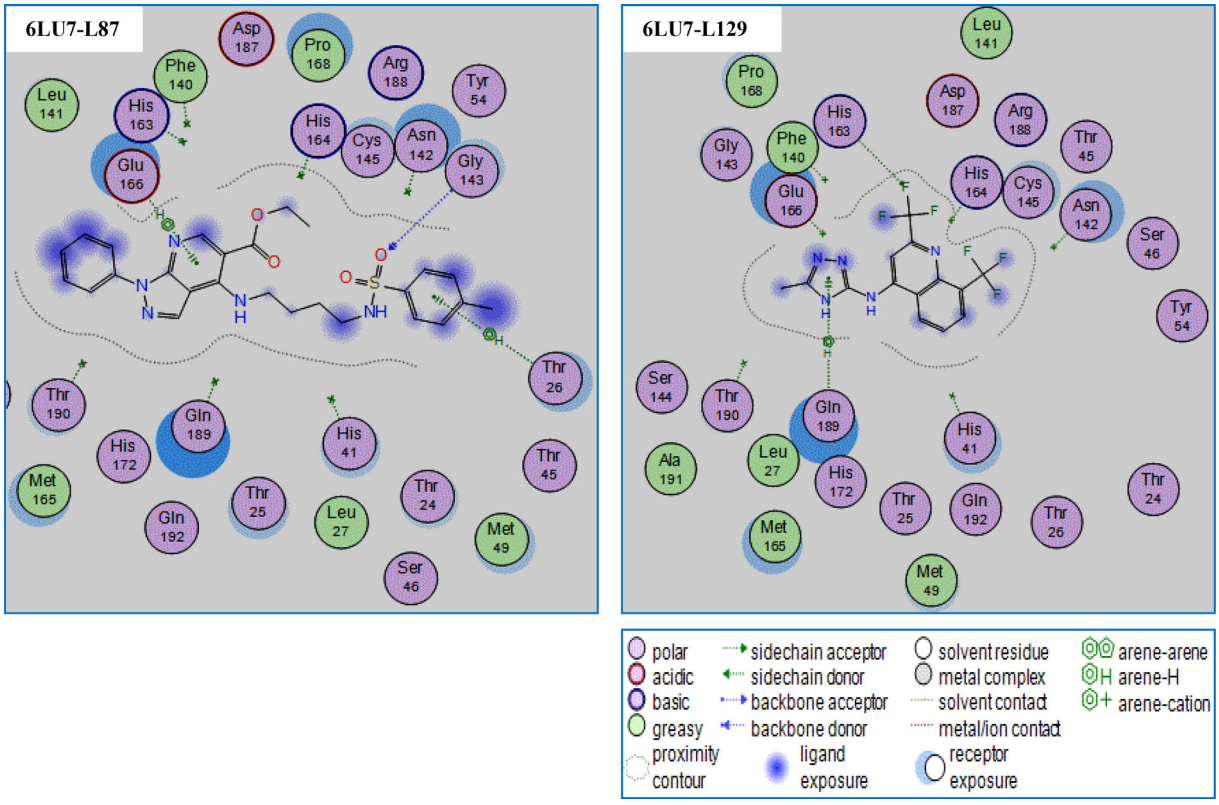

Figure 3. Detailed view of both compounds L87 and L129 binding in the active site of the enzyme (enzyme PDB: 6LU7).

such as, blood–brain partitioning (Norinder & Haeberlein, 2002), human intestinal absorption (Fagerholm, 2007; Hou et al., 2008; Johnson & Zheng, 2006), oral bioavailability (Johnson & Zheng, 2006), Caco-2 permeability (Norinder & Bergström, 2006; Hou et al., 2006), P-glycoprotein-mediated transport (Ekins et al., 2007), volume of distribution, clearance, even half-life, plasma-protein binding (Van De Waterbeemd & Gifford, 2003), metabolism (Jolivette & Ekins, 2007) and including solubility (Delaney, 2005). Meanwhile, ADME properties software was used to predict a range of ADME properties, among them SwissADME (Daina et al., 2017).

5. Results and discussion

5.1. Docking and pose analysis

For generating and evaluating the compounds conformations with targets you have to choose a good search algorithm and scoring function, this depends on the software used in the molecular docking simulation. A molecular docking calculation is evaluated by two parameters, energy score (calculated by scoring function) and bonds (calculated by search algorithm) between the compounds and active site residues of all the targets.

The details results of docking calculations and the best pose received after a docked of all compounds with SARS-CoV-2, SARS-CoV and MERS-CoV targets are listed in Table 2.

5.1.1. SARS-CoV-2-compounds interactions

The results obtained show that the score of binding free energy of all complexes (6LU7-Compunds) was between −5.392 and −7.607 kcal/mol and the complexes forming by compounds: L87 and L129 have the lowest binding energy score compared to the other complexes (see Figure 3; Figure 3a, supplementary material). They give the best docking scores, based on the binding free energy, citing here: **−7.607** and −6.920 respectively (Table 2). This shows that these complexes are more stable.

We note that the complex formed by the compound L87 (6LU7-L87) (Figure 2 (a,b)) has the lowest energy score compared to the other complexes formed by clinical test. Moreover, this compound forms three interactions with active site residues. In addition, this compound formed three interactions with active site residues of the SARS-CoV-2 target.

The complex formed by compound L129 gave a score value very close (slightly higher) to the value of the both best of clinical test Remdesivir and Arbidol (Table 2, see supplementary material) which theirs binding free energy was −7.357 and −7.102 kcal/mol respectively. In addition, this compound establishes two interactions with active site residues of the SARS-CoV-2 target.

The binding mode observed for compound L87 shows that it establishes three interactions with the receptor pocket, Two interactions pi-H does appear in Figure 3, the first one between 6-ring of a compound and N atom of THR26 (4.41 Å), the second between 5-ring of compounds and N atom of GLU166(4.15 Å), the third is the type H-acceptor formed between the O-18 atom of a compound and N atom of GLy143 (3.02 Å) (Table 2), and according to Imberty et al. (1991), interactions between 2.5 Å and 3.1 Å are considered strong and those between 3.1 Å and 3.55 Å

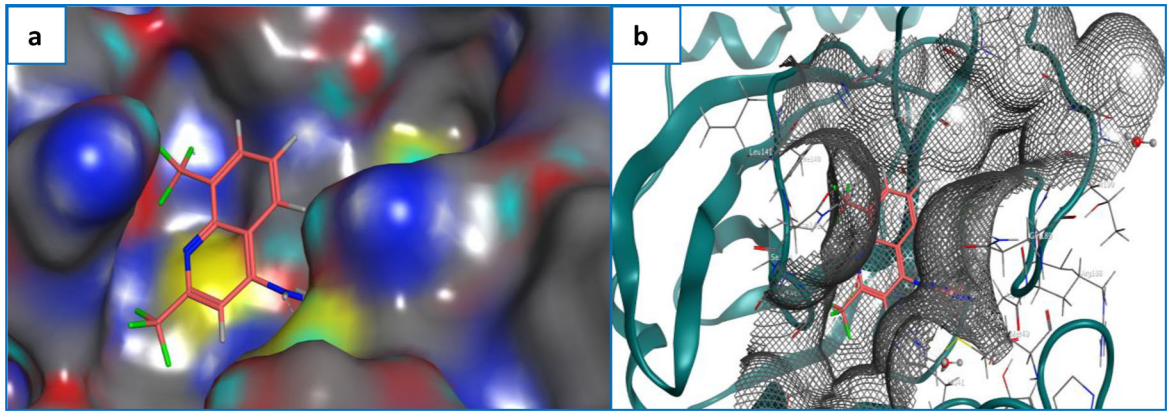

Figure 4. (a) The top scoring compound. (b) A novel inhibitor L-129 identified by molecular docking is shown in the active site.

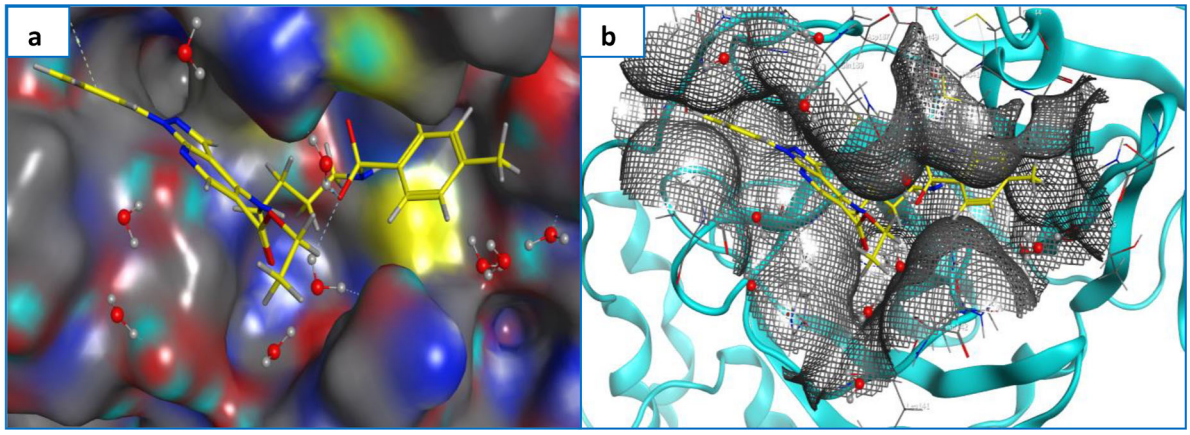

Figure 5. (a) The top scoring compound. (b) A novel inhibitor L-87 identified by molecular docking is shown in the active site.

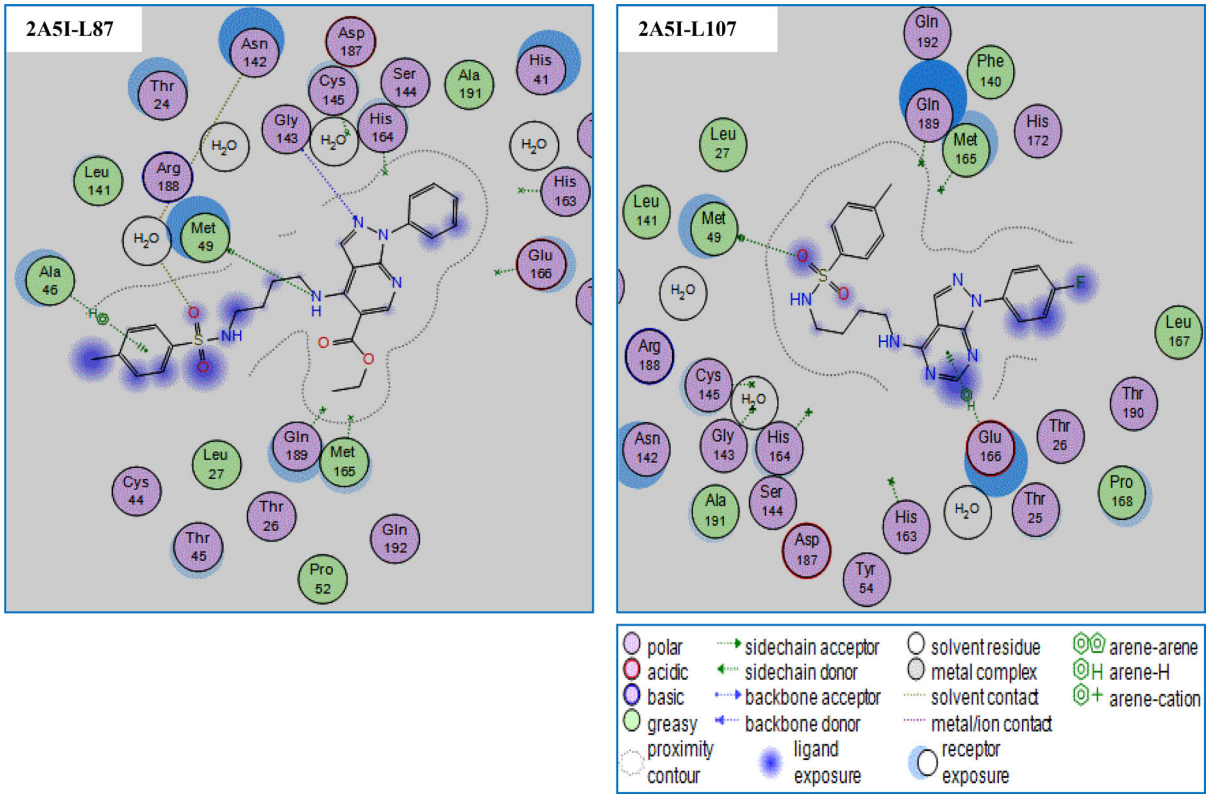

Figure 6. Detailed view of both compounds L87 and L107 binding in the active site of the enzyme (enzyme PDB: 2A5I).

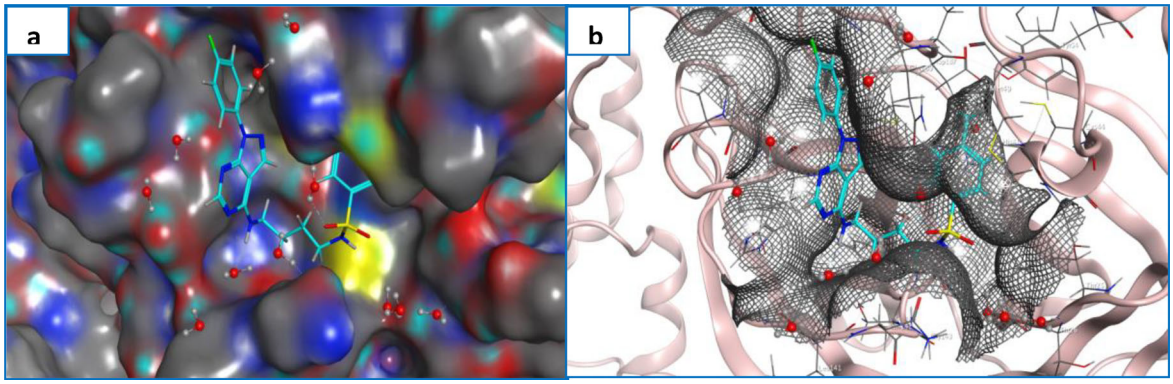

Figure 7. (a) The top scoring compound. (b) A novel inhibitor L-107 identified by molecular docking is shown in the active site.

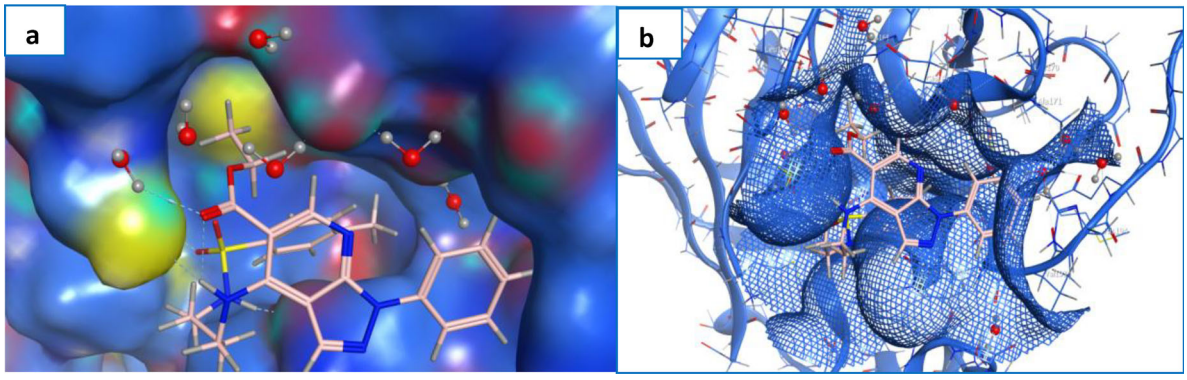

Figure 8. (a) The top scoring compound. (b) A novel inhibitor L-87 identified by molecular docking is shown in the active site.

are assumed to be weak. This confirms that this H-acceptor obtained is strong. In the other hand, these results obtained by docking the molecules are confirmed by the good inhibition against Malaria (IC50 = 3.46 μM) of this compound (Luiz et al., 2019). Similarly compound L129 is most active towards Malaria (IC50 = 0.083 μM) also the complex formed by this compound give low score energy and establish two interactions with the active site residues. The first one is H-acceptor (2.94 Å) between F-27 of a compound and NE2 of HIS163. The second interaction pi-H (4.68) formed between 5-ring of compound and the CG of GLN189. This H-acceptor (2.94 Å) is strong, according to Imberty et al. (1991).

5.1.2. SARS-CoV-compounds interactions

The results obtained show that the score of binding free energy of all complexes (2A5I-Compunds) was between −5.595 and −8.764 kcal/mol and the complexes forming by compounds: L87 and L107 have the lowest score of binding energy compared to the other complexes (see Figure 6; Figure 6a, supplementary material). They give the best docking scores, based on the binding free energy, citing here: **−8.764** and −7.309 respectively (Table 2). This shows that these complexes are more stable. The complex formed by compound L87 gives the lowest score energy values 8.764 compared to the all complexes which that formed by clinical test. This compound establishes four interactions with the active site residues of the receptor (Figure 6). However, the compounds L87 is revealed good inhibition against Malaria (IC50 = 3.46 μM).

The complex formed by compound L107 (Figure 7 (a,b)) gave a very close score value (slightly higher) to the best clinical test Remdesivir and Arbidol score values (Table 2, see supplementary material). Whereas, their bindings free were: −8.204 and −7.381 kcal/mol respectively. In addition, this compound establishes two interactions with the active site residues of the target.

In Figure 6, we observe that compound L87 establishes four interactions with pocket of receptor, Two interactions H-acceptor, the first one, between N-11 of compound and N atom of GLY143(3.63 Å), the second between O-29 of a compound and O atom of HOH538(3.24 Å), the third is the type H-donor formed between the N-17 atom of a compound and SD atom of MET49 (3.99 Å), and the last pi-H formed between 6-ring of the compound and N atom of ALA46(4.62 Å) (Table 2), and according to Imberty et al. (1991), all these H-Bond (acceptor and donor) obtained are weak. Similarly compound L107 give low score energy and establish two interactions with the active site residues. The first one is H-donor (3.87 Å) between O-23 of a compound and SD of MET49. The second interaction pi-H (4.10 Å) formed between 6-ring of compound and the CB of GLU166. This H-donor is weak according to Imberty et al. (1991). This compound was known to have a good inhibition against Malaria (IC50 = 5.13 μM) (Luiz et al., 2019).

5.1.3. MERS-CoV-compounds interactions

The results obtained show that the binding free energy score of all complexes (5WKK-Compounds) was between −5.400

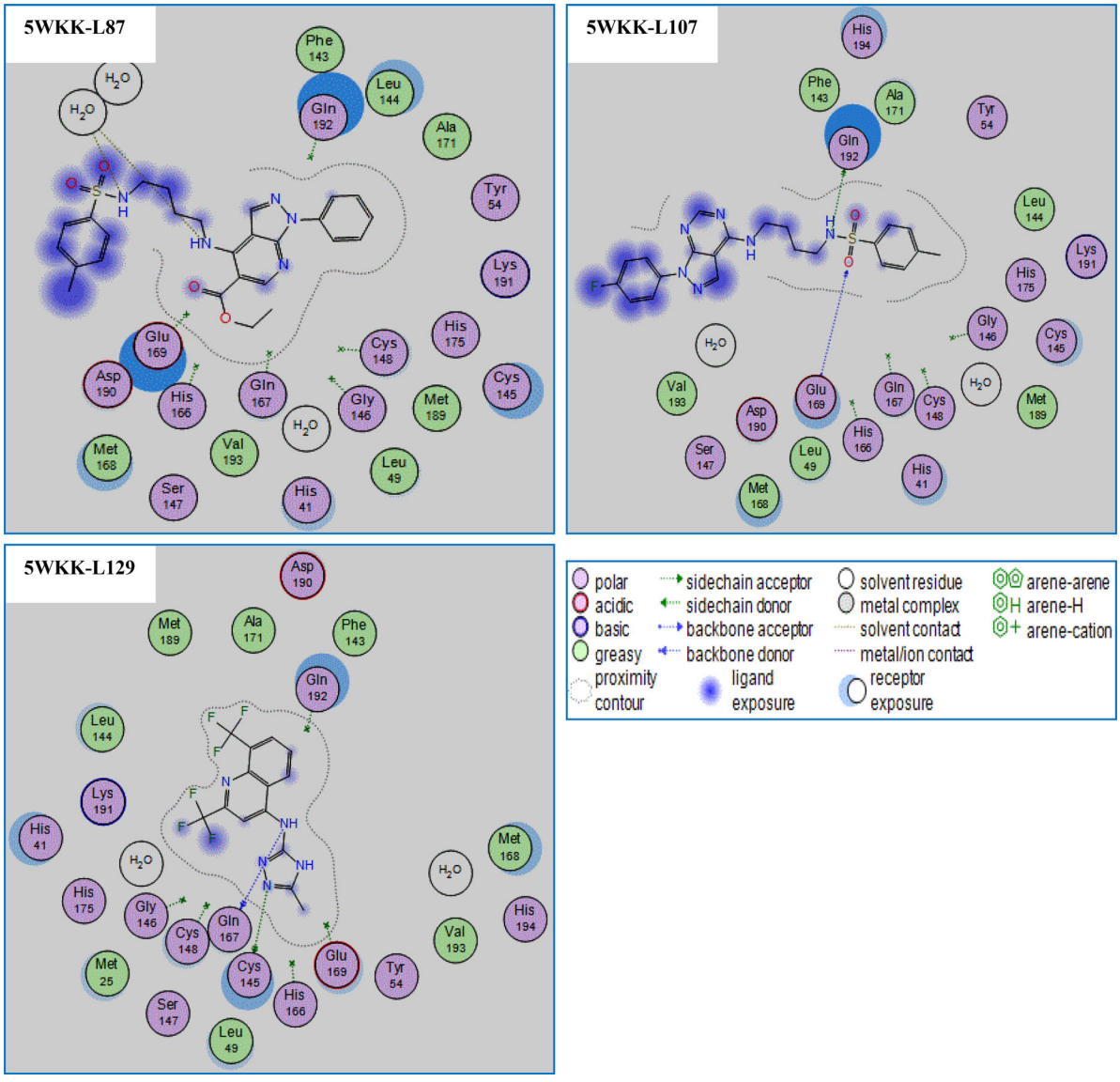

Figure 9. Detailed view of both compounds L87, L107 and L129 binding in the active site of the enzyme (enzyme PDB: 5WKK).

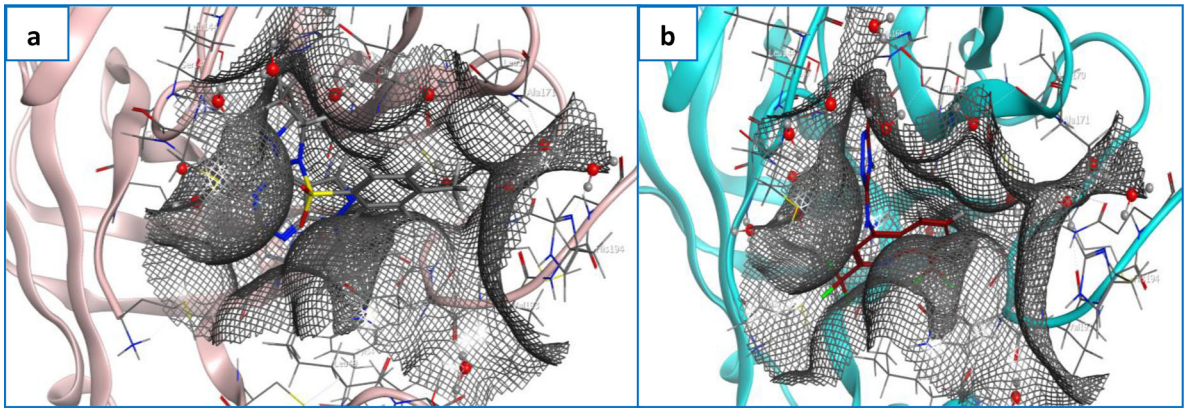

Figure 10. (a) The top scoring compound, L107. (b) A novel inhibitor L-129 identified by molecular docking is shown in the active site.

and −7.074 kcal/mol and the complexes forming by compounds: L87, L107 and L129 have the lowest binding energy scores compared to the other complexes. They give the best docking scores, based on the binding free energy, citing here: −7.074, −6.759 and −6.686 respectively (Table 2) (see Figure 9; Figure 9a, supplementary material). This shows that these complexes are more stable. The complex formed by the compound L87 (Figure 8 (a,b)) gives a low energy value of the score −7.074 kcal/mol that it is very close to the value of the clinical test, Remdesivir and Arbidol (Table 2; Figure

9b, supplementary material), this compound establishes two interactions with the residues of active sites of MERS-CoV (Figure 9). On the other hand, we note that the compound L87 considered among the most powerful compounds for the inhibition of Malaria (IC50 = 3.46 μM).

Similarly, compounds L107 and L129 (Figure 10 (a,b)) have low energy score values −6.759 and −6.686 kcal/mol respectively (Table 2). They are involved in making two interactions with the active site residues.

Figure 5 shows that compound L87 establishes two strong H-donor interactions with receptor pocket, the first one, between O-17 of a compound and O atom of HOH517(3.11 Å), the second between N-26 of a compound and O atom of HOH517(2.99 Å) (Table 2).

Compound L107 is making two interactions with the receptor pocket (Figure 6), the first one, strong H-donor interaction (3.00 Å) between N-21 of a compound and OE1 atom of GLY192, the second, weak H-acceptor interaction (3.37 Å) between O-24 of a compound and N atom of GLU169, similarly compound L129 is making two H-donor interactions with receptor active site residues, The first one is strong between N-11 of a compound and O of GLN167(3.07 Å). The second is weak formed between N-14 of compound and the SG of SYS145 (3.26 Å) (Table 2).

Table 3. Thermodynamic properties calculated in reels units. Pressure P = P* ε/ σ^{-3}, Energy of configuration U = U* Nε, translation Kinetic Energy EKT = EKT* Nε and Enthalpy H = H* Nε.

SP_i	Method	H	U	EKT	P
SPi	SARSCOV-2-Lig-87	0.2563	542.365	2532.256	−42.236
	SARS-COV-Lig-87	0.2745	742.326	1452.365	−40.526
	MERS-Lig-87	1.542	956.256	1452.325	−35.265
	SARSCOV-2-Lig-107	0.352	752.365	1542.365	−25.365
	SARS-COV-Lig-107	0.745	865.256	2563.212	−28.256
	MERS-Lig-107	0.542	1025.002	2453.254	−24.256

5.2. MD simulation analysis

Many previous studies (Chen et al., 2014, Chen, 2015; Huang et al., 2014; Hung et al., 2014) confirmed that the highest dock score obtained by molecular docking does not mean that the compound is a potent lead, but, to validate this result it is necessary to be accompanied by molecular dynamics simulations.

The molecular dynamics results are grouped together in Table 3 for the selected compounds L87 and L107. The production MD phase was carried out at 300 K for 100 ns with a time step of 1 fs using the constant volume and temperature (NVT) ensemble.

In contrast to the complex formed by L87 their energies (Energy of configuration and translation Kinetic Energy) were low (Figures 11–13) shows significant pressure fluctuations for the complex formed by L107 with an order of: 0. 024–0.035 which explains the instability of the system, therefore, the rotational movement and vibration energy is important oscillation. Therefore, the L87 is predicted to be the most interactive system. These results are in total agreement with the Molecular Docking results (Table 2). The curves of both complexes 6LU7-L87 and 6LU7-L107 show that after 600 ps there is the stability of the potential energy (Figure 4) and both compounds L87 and L107 create the same number of interactions with the active site residues of

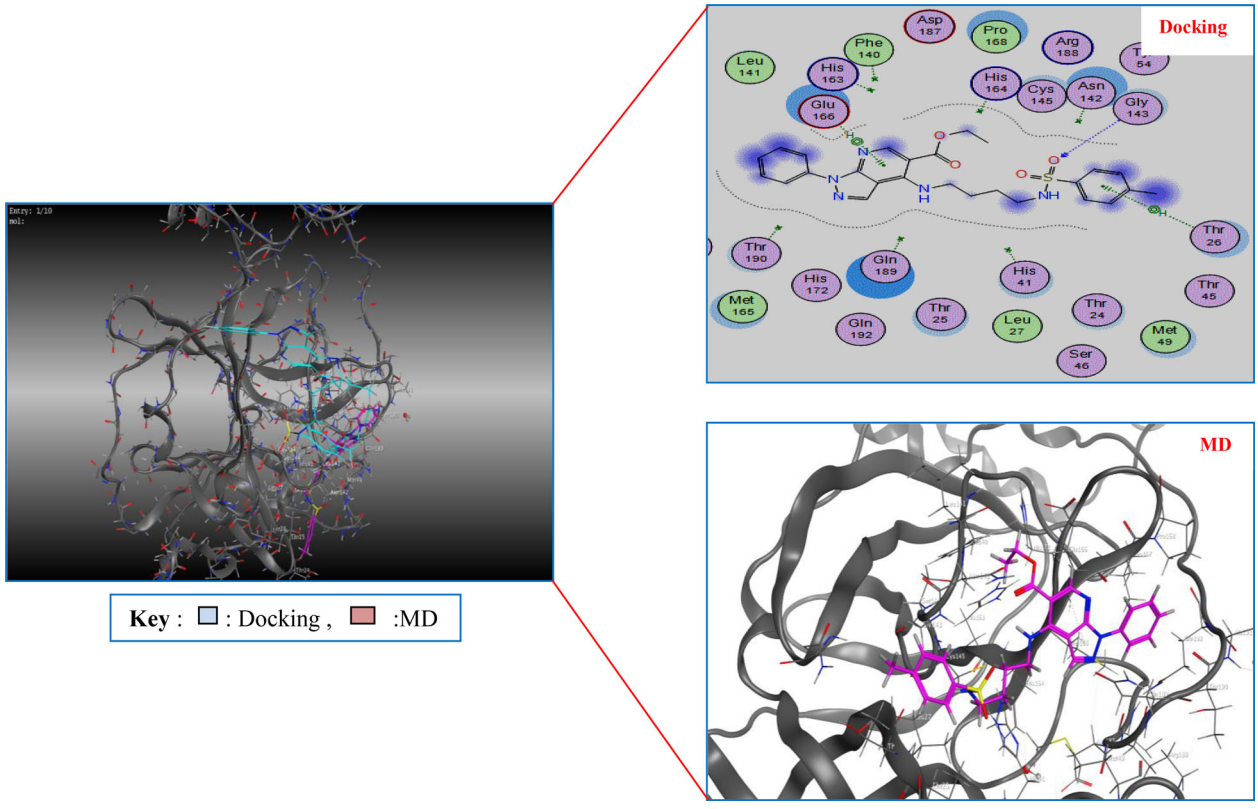

Figure 11. The compound L87 is docked without water well into the binding site of **SARS-COV2** and has the highest dock score; there is also a clear difference between the final ligand pose and the docking pose after a molecular dynamics (MD) simulation.

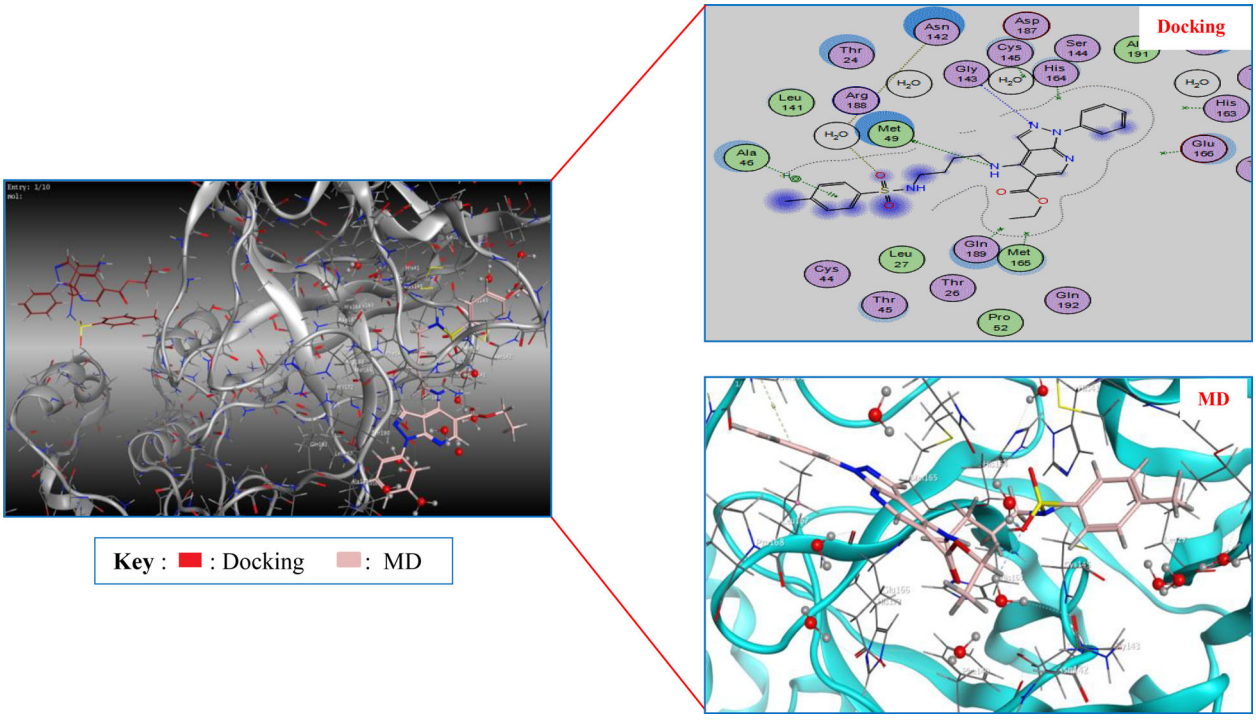

Figure 12. The compound L87 is docked without water well into the binding site of **SARS-COV** and has the highest dock score; there is also a clear difference between the final ligand pose and the docking pose after a molecular dynamics (MD) simulation.

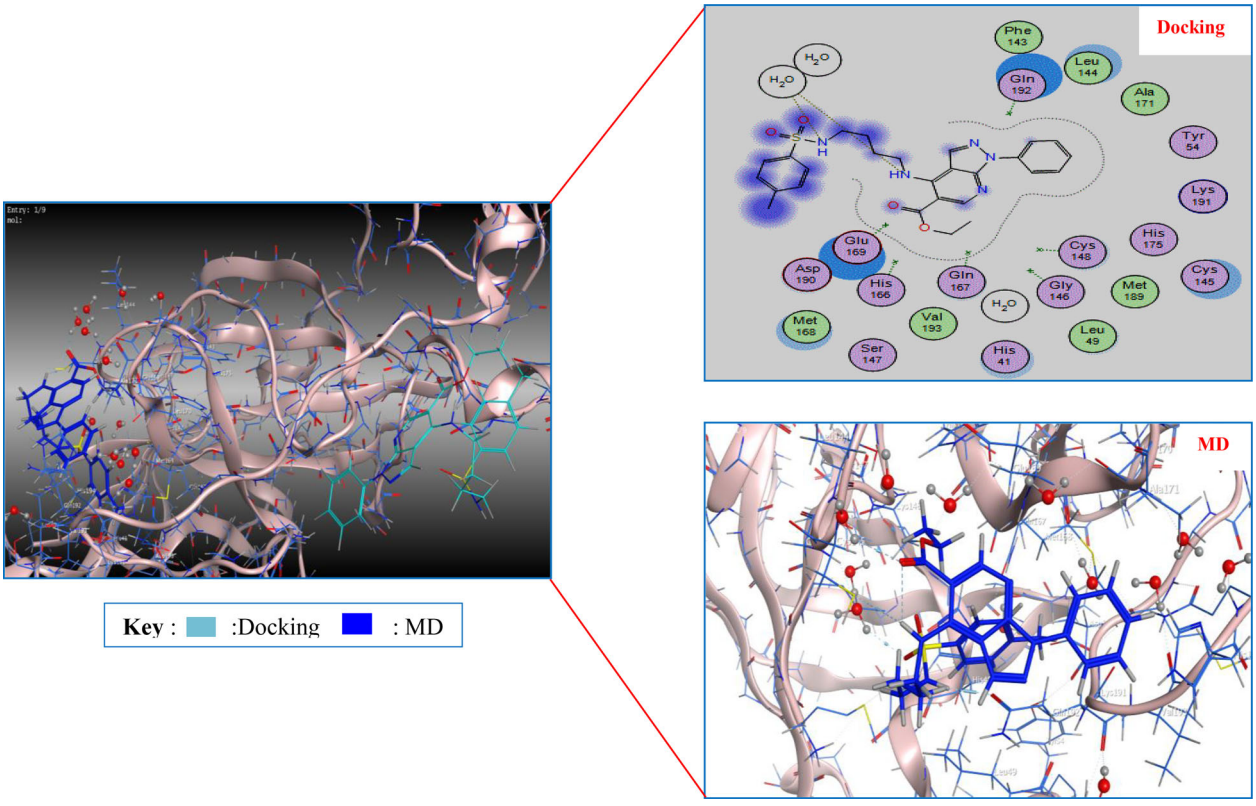

Figure 13. The compound L87 is docked without water well into the binding site of **MERS-COV** and has the highest dock score; there is also a clear difference between the final ligand pose and the docking pose after a molecular dynamics (MD) simulation.

the SARS-CoV compared to molecular docking calculation but with other active site residues. In the last case, we can see that the three complexes 5WKK-L87, 5WKK-L107 and 5WKK-L129 show that after 800 ps there is a stability of the potential energy (Figure 4) and both compounds L87 and L129 establishes the same number of interactions with the same active site residues of MERS-CoV compared to molecular docking calculation but the compound L107 forms the

Table 4. ADME properties for three top scoring lead compounds of SARS-CoV-2, SARS-CoV and MERS-CoV targets.

						Rules		
Compounds	n-ROTB	MW	Log P	n-ON acceptors	n-OHNH donors	Lipinski's violations	Veber violations	Egan violations
	–	**<500**	**≤5**	**<10**	**<5**	**≤1**	**≤1**	**≤1**
L87	12	507.60	2.87	7	2	0	0	0
L107	9	454.52	2.99	7	2	0	0	0
L129	4	361.25	3.15	9	2	0	0	0

Table 5. Pharmacokinetics and Medicinal Chemistry properties for all compounds.

	Pharmacokinetics		Medicinal Chemistry	
Molecules	*GI absorption*	*Log K_p (skin permeation)*	*Leadlikeness*	*Synthetic accessibility*
L2	Low	−9.56 cm/s	No; 1 violation: MW > 350	6.43
L44	Low	−10.12 cm/s	No; 1 violation: MW > 350	6.34
L56	High	−5.66 cm/s	Yes; 0 violation:no alerts 0 MW < 350	2.98
L75	High	−5.05 cm/s	No; 3 violations: MW > 350, Rotors > 7, XLOGP3 > 3.5	2.76
L83	Low	−3.57 cm/s	No; 3 violations: MW > 350, Rotors > 7, XLOGP3 > 3.5	4.47
L87	**Low**	**−5.85 cm/s**	**No; 3 violations: MW > 350, Rotors > 7, XLOGP3 > 3.5**	**3.71**
L107	**High**	**−6.23 cm/s**	**No; 3 violations: MW > 350, Rotors > 7, XLOGP3 > 3.5**	**3.26**
L129	Low	−5.79 cm/s	No; 2 violations: MW > 350, XLOGP3 > 3.5	2.56

interactions with other active site residues. Finally, this means that the complexes formed by these compounds are better stable in molecular dynamics because hydrogen interactions are stronger compared to the other interactions (Jaworski et al., 2016; Robertson et al., 2017; Varadwaj et al., 2019; Xie et al., 2015; Xu et al., 2018).

5.3. In silico evaluation of the ADME properties and drug-likeness

A computational study of three top scoring lead compounds was performed for assessment of ADME properties and the obtained value is depicted in Table 4.

The results presented in Table 6 revealed that compound L107 have high absorption and both compounds L87 and L129 have low absorption. Also, can be observed that all compounds comply with Lipinski's rule of 5, Veber and Egan where log*P* values ranged between 2.87–3.15 (<5), MW range 292–478 (<500), HBA range 7–9 (≤10) and HBD range 2–2 (<5), suggesting that these compounds would not be expected to cause problems with oral bioavailability and thus showing possible utility of all these compounds for developing the compound with good drug like properties against Covid-19.

The results Medicinal Chemistry and Pharmacokinetics showed that compound L87 and compound L129 have Low GI absorptions. We notice that there is a correlation between our results found by the predicted results in medicinal chemistry and pharmacokinetics (Table 5).

Compound 107 is predicted to be characterized by a high lipophilicity and high coefficient of skin permeability log Kp by providing L87 and L129. We can conclude that the more negative the log Kp (with Kp in cm/s), the less the molecule is permeable to the skin which explains the reliability of our results. Therefore, compound L87 represents high affinity with three targets. Synthetic accessibility (SA) is a major factor to take into account in this selection process an acceptable value between 3.26 and 3.71 for the compound (L107 and L87) respectively, these are more promising molecules which can be synthesized or subjected to bioassays or other experiments. According to its pharmacokinetic properties (Figure 14) Compound 107 showed a high level of gastrointestinal adsorption which contributes to *good oral* bioavailability.

Compound L87 has a maximum of 2H + donors and 7 H + acceptor atoms, as shown in (Figure 12). According to its pharmacokinetic properties, compound L87 showed a low level of gastrointestinal adsorption which contributes to bad oral bioavailability. But, *inhaled*.

Compound L87 according to pharmacokinetic parameters evaluated in silico showed no inhibition of cytochrome P450 isomers 1A2.

Compound L107 has a maximum of 2H + donors and 7 H + acceptor atoms, as shown in (Figure 11). According to its pharmacokinetic properties, ligand107 showed a high level of gastrointestinal adsorption (Table 5) which contributes to *good oral* bioavailability.

Compound L107 can inhibit CYP1A2, which might cause a potential interference with the metabolism of other concomitantly administered herbs or drugs; it may alter the metabolism of drugs by CYP. However, it should be noted that inhibition of CYP1A2 activity *in vitro* does not necessarily imply drug interaction *in vivo*. Further studies will be needed to determine if this L04 can influence the CYP enzyme *in vivo*.

5.4. Pharmacophore mapping

PharmMapper Server is accessed web-server designed to identify potential target candidates for the given probe small molecules (drugs, natural products, or other newly

Table 6. Results of the P450 sites of metabolism prediction study of the best compounds.

Names of P450 isoenzymes	**Compound 87** *Ethyl 4-((4-(4-methylphenylsulfonamido) butyl)amino)-1phenyl-1H-pyrazolo [3,4-b]pyridine-5-carboxylate*	Names of P450 isoenzymes	**Compound 87** *Ethyl 4-((4-(4-methylphenylsulfonamido) butyl)amino)-1phenyl-1H-pyrazolo [3,4-b]pyridine-5-carboxylate*
1A2	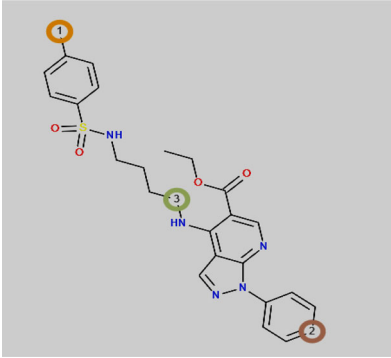	2C8	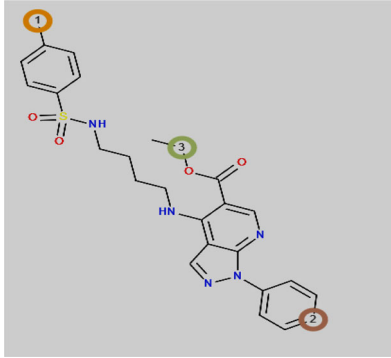
2A6	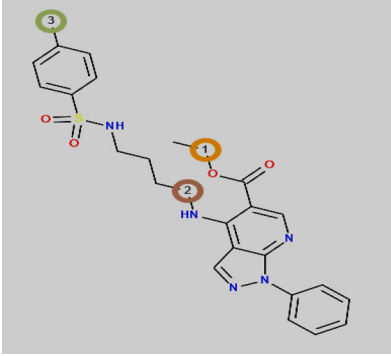	2C9	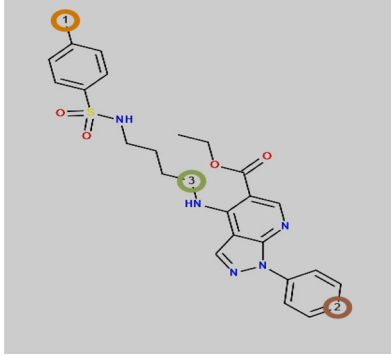
2B6	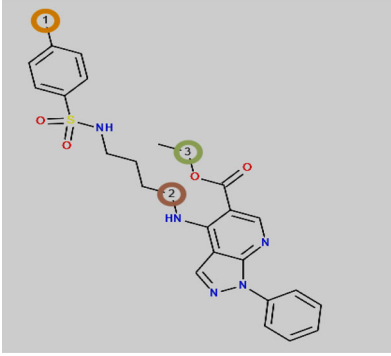	2C19	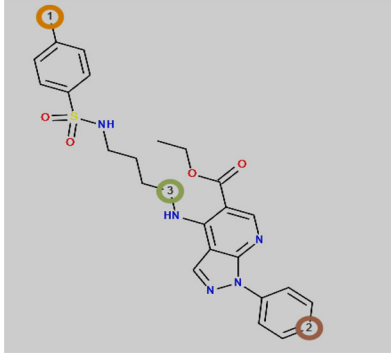
2D6	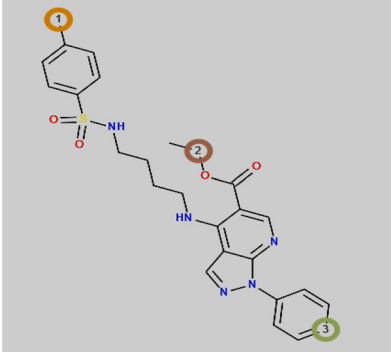	2E1	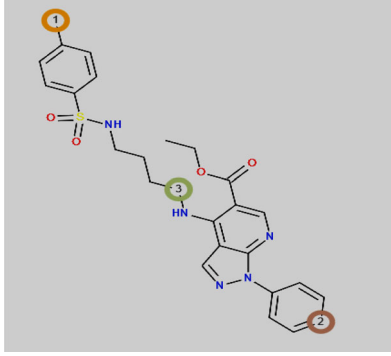

discovered compounds with binding targets unidentified) using pharmacophore mapping approach (Liu et al., 2010; Wang et al., 2016, 2017). The possible sites of metabolism by CYPs 1A2, 2A6, 2B6, 2C19, 2C8, 2C9, 2D6, 2E1 and 3A4 of the best compound L87 was summarized in Table 6. The possible sites of the studied compound, where the metabolism of CYP450 enzymes isoforms may be taken place, are illustrated by circles on the chemical structure of the molecule (Zaretzki et al., 2013). Thus, we can say that the compound L87 can be metabolized by these enzymes.

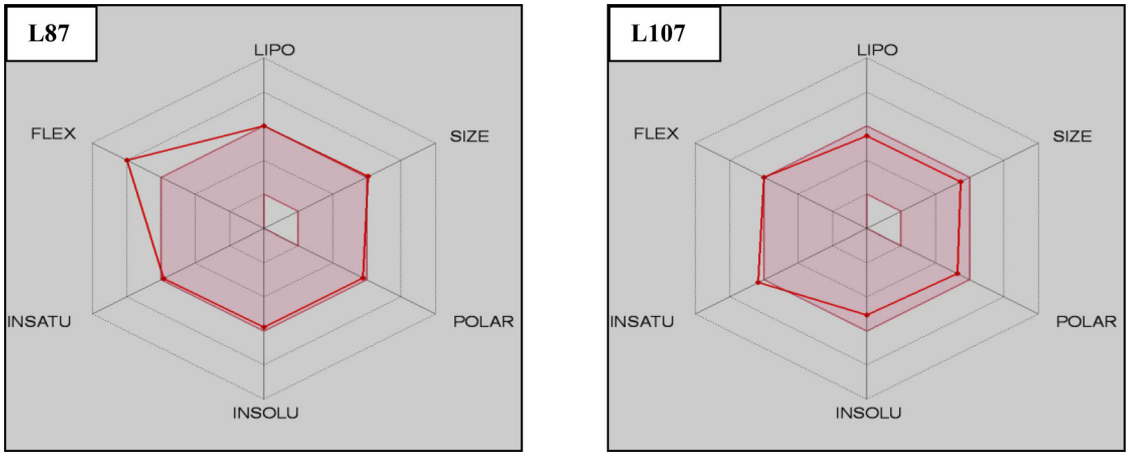

Figure 14. Biovailability and pharmacokinetic parameters for too compounds L87 and L107 using Swiss ADME (www.SwissADME.ch).

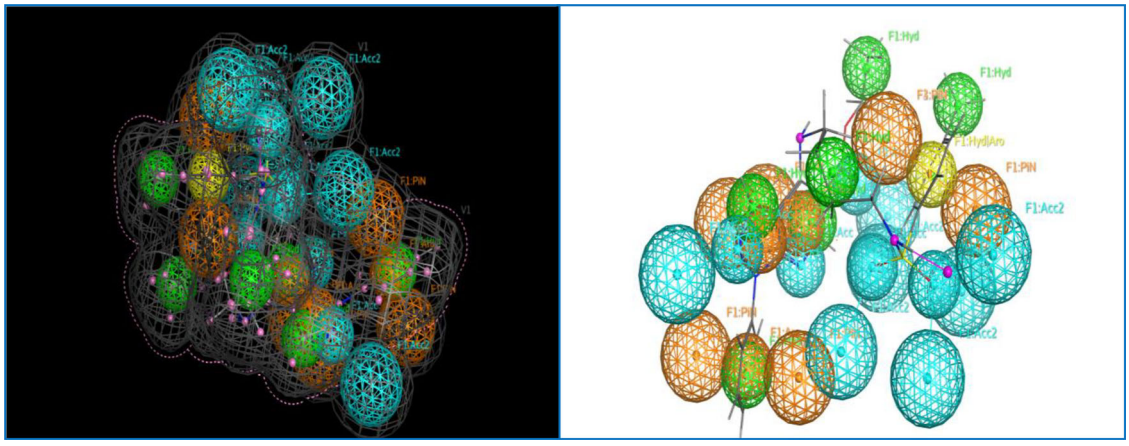

Figure 15. Pharmacophore Mapping of compound L87. Here, cyan color—hydrogen bond acceptor, orange color—aromatic, green color—hydrophobic.

The P450 SOM predictions showed that compound L87 had 3sites of metabolism (SOMs) for the CYP 450 1A2, 450 2A6 enzyme, CYP 450 2B6, CYP 450 2D6, CYP 450 2C8, CYP 450 2C9, CYP 450 2C19 and CYP 450 2E1.

The pharmacophore Mapping is conveyed for the compound L87 best *inhaled* ligand, showed for L87, 2 hydrogen acceptor bonds, 6 Hydrophobic groups and 9 Aromatic rings. It also generated a good number of good contacts with the pharmacophore of three targets SARS-CoV-2, SARS-CoV and MERS-CoV (Figure 15).

The pharmacophore of compound L87 generates a hypothesis which can be applied successfully in biological screening for further experiments (Dixon et al., 2006).

Here, cyan color-hydrogen bond acceptor, orange color-aromatic, green color-hydrophobic Validation of our results, formed with SARS-CoV-2 under Clinical test is mentioned in (Table 7).

Silva et al. synthesized and assayed Ten derivatives of 1-phenyl-1H-pyrazolo [3,4-b] pyridine against Plasmodium falciparum. The compound L87 the best ligand in our search (Ethyl 4-((4-(4-methylphenylsulfonamido) butyl) amino)-1phenyl-1H-pyrazolo [3,4-b] pyridine-5-carboxylate) was among these ten compounds. The latter exhibited in vitro activity against the Chloroquine resistant clone W2 with IC50 values ranging from 3.46 to 9.30 μM. Therefore, the 1Hpyrazolo [3,4-b] pyridine system is considered to be antimalarial (Silva et al., 2016).

Finally, our obtained results showed that the compound L87 (*Ethyl 4-((4-(4-methylphenylsulfonamido)butyl)amino)-1phenyl-1H-pyrazolo[3,4-b]pyridine-5-carboxylate)* can be used as a potential agents to treat COVID-19 if we comparing to Chloroquine, Hydroxychloroquin, Remdesivir, Arbidol antiviral drugs and it can emerge as the most potent anti-ACE2 agent.

6. Conclusion

During our research on new drugs for Covid-19 treatment, we used three computational methods: molecular docking analyzes MD simulations and ADME properties, to test the affinity of a new class of compounds obtained from hybridization of clinical test drugs with three enzymes SARS-CoV-2, SARS-CoV and MERS-CoV.

Our top three compounds showed high binding affinities and many binding interactions with the studied targets in the molecular docking simulation. However, molecular dynamic calculations were used to confirm and validate our docking simulation results in order to study the stability of

Table 7. Energy balance of complexes formed with SARS-CoV-2 under Clinical test and Our Results.

Molecule	Score		References
		6lu7 was received in the PDB database (Choudhary et al., 2020)	
		SARS-COV-2	
Lref (Native) PRD_002214		**−10.67087121**	
		Clinical test	
	SARS-COV-2	**Number of interactions**	
Chloroquine	−5.918	2 Hydrogen-bond formed with: HIS41 and MET49	(Keyaerts et al., 2004; Luiz et al., 2019; Narkhede et al., 2020; Vincent et al., 2005)
Hydroxychloroquine	−5.959	1 Hydrogen-bond formed with: ASN151	(McChesney, 1983; Narkhede et al., 2020)
Remdesivir	−7.357	2 Hydrogen-bond formed with: PHE294 and GLN110 2 Pi-Segma bond formed with: ILE249 and VAL104	(Narkhede et al., 2020; Warren et al., 2016)
Arbidol	−7.102	2 Hydrogen-bond formed with: CYS336, SER371and PHE338 2 Pi-Pi bond formed with: TRP436	(Abouelela et al., 2021; Narkhede et al., 2020; Panisheva et al., 1988)
Favipiravir	−3.492	6 Hydrogen bonds with: GLN 110, THR 292, THR 111, ASP 295 and ASN 151	(Abouelela et al., 2021; Furuta et al., 2005; Narkhede et al., 2020)
Ribavirin	−5.447	4 Hydrogen-bond formed with: TYR239, TYR237, ARG131 and ARG131	(Abouelela et al., 2021; Narkhede et al., 2020; Witkowski et al., 1972)
Sofosbuvir	−6.606	/	(Bullard-Feibelman et al., 2017)
Amodiaquine	−6.402	/	(Luiz et al., 2019)
Mefloquine	−5.786	/	
Our results			
L87	−7.607	1 Hydrogen-bond formed with: Gly143 2 Pi-H bond formed with: GLU166 and THR26	/
L107	−6.338	1 Pi-H bond formed with: GLU166	/
L129	−6.920	1 Hydrogen-bond formed with: HIS163 1 Pi-H bond formed with: GLN189	/

the formed complexes between our compounds (L87, L107 and L129) and the active site residues of SARS-CoV-2, SARS-CoV and MERS-CoV targets. The obtained results, according to the binding interactions, show a stable state under dynamic conditions. In addition, we found that three top candidates established many interactions with SARS-CoV-2, SARS-CoV and MERS-CoV targets which gives a higher affinity and a low binding energy with these targets. At the end, the combined study between molecular docking and dynamics proves that we can consider compounds L87, L107 and L129 the best inhibitors against the SARS-CoV-2, SARS-CoV and MERS-CoV targets. Moreover, these compounds respect the Lipinski, Veber and Egan rules. Also, the Pharmacokinetics of L87 was justified by means of lipophilicity and high coefficient of skin permeability. Finally, we can say that these results allow us to select compound L87 can be further developed as an oral drug candidate against the pandemic of Covid-19.

Acknowledgements

Authors thank the Algerian Ministry of Higher Education and Scientific Research for the support under the PRFU project (approval No. B00L01UN130120190009). The authors thank director of Laboratory—LASNABIO Pr Said GHALEM for his financial support and ensure that there is no conflict of interest regarding this paper.

Disclosure statement

The authors declare no potential conflicts of interest with respect to the research, authorship, and/or publication of this article.

References

Abouelela, M. E., Assaf, H. K., Abdelhamid, R. A., Elkhyat, E. S., Sayed, A. M., Oszako, T., Belbahri, L., El Zowalaty, A. E., & Abdelkader, M. S. A. (2021). Identification of potential SARS-CoV-2 main protease and spike protein inhibitors from the genus aloe: An in silico study for drug development. *Molecules*, *26*(6), 1767. https://doi.org/10.3390/molecules26061767

Alamri, M. A., Tahir Ul Qamar, M., & Alqahtani, S. M. (2020). Pharmacoinformatics and molecular dynamic simulation studies reveal potential inhibitors of SARS-CoV-2 main protease 3CLpro. *Journal of Biomolecular Structure and Dynamics*, *39*(13), 4936-4948. https://doi.org/10.1080/07391102.2020.1782768

Arnold, K., Bordoli, L., Kopp, J., & Schwede, T. (2006). The SWISS-MODEL workspace: A web-based environment for protein structure homology modelling. *Bioinformatics (Oxford, England)*, *22*(2), 195–201. https://doi.org/10.1093/bioinformatics/bti770

Aryapour, H., Dehdab, M., Sohraby, F., & Bargahi, A. (2017). Prediction of new chromene-based inhibitors of tubulin using structure-based virtual screening and molecular dynamics simulation methods. *Computational Biology and Chemistry*, *71*, 89–97. https://doi.org/10.1016/j.compbiolchem.2017.09.007

Azam, M. A., & Jupudi, S. (2017). Extra precision docking, free energy calculation and molecular dynamics studies on glutamic acid derivatives as MurD inhibitors. *Computational Biology and Chemistry*, *69*, 55–63. https://doi.org/10.1016/j.compbiolchem.2017.05.004

Ballu, S., Itteboina, R., Sivan, S. K., & Manga, V. (2018). Rational design of methicillin resistance staphylococcus aureus inhibitors through 3D-QSAR, molecular docking and molecular dynamics simulations. *Computational Biology and Chemistry*, *73*, 95–104. https://doi.org/10.1016/j.compbiolchem.2017.12.007

Beigel, J. H., Tomashek, K. M., Dodd, L. E., Mehta, A. K., Zingman, B. S., Kalil, A. C., Hohmann, E., Chu, H. Y., Luetkemeyer, A., Kline, S., Lopez de Castilla, D., Finberg, R. W., Dierberg, K., Tapson, V., Hsieh, L., Patterson, T. F., Paredes, R., Sweeney, D. A., Short, W. R., … Lane, H. C. (2020). Remdesivir for the treatment of Covid-19. *New England Journal of Medicine*, *383*(19), 1813–1826. https://doi.org/10.1056/NEJMoa2007764

Berendsen, H. J., Postma, J. V., van Gunsteren, W. F., DiNola, A. R., & Haak, J. R. (1984). Molecular dynamics with coupling to an external bath. *The Journal of Chemical Physics*, *81*(8), 3684–3690. https://doi.org/10.1063/1.448118

Bond, S. D., Benedict, J. L., & Laird, B. B. (1999). The Nosé-Poincaré Method for Constant Temperature Molecular Dynamics. *Journal of Computational Physics*, *151*(1), 114–134. https://doi.org/10.1006/jcph.1998.6171

Bosch, B. J., van der Zee, R., de Haan, C. A., & Rottier, P. J. (2003). The coronavirus spike protein is a class I virus fusion protein: Structural and functional characterization of the fusion core complex. *Journal of Virology*, *77*(16), 8801–8811. https://doi.org/10.1128/jvi.77.16.8801-8811.2003

Bourouiba, L. (2020). Turbulent gas clouds and respiratory pathogen emissions: Potential implications for reducing transmission of COVID-19. *JAMA*, *323*(18), 1837-1838. https://doi.org/10.1001/jama.2020.4756

Bullard-Feibelman, K. M., Govero, J., Zhu, Z., Salazar, V., Veselinovic, M., Diamond, M. S., & Geiss, B. J. (2017). The FDA-approved drug sofosbuvir inhibits Zika virus infection. *Antiviral Research*, *137*, 134–140. https://doi.org/10.1016/j.antiviral.2016.11.023

Calina, D., Docea, A. O., Petrakis, D., Egorov, A. M., Ishmukhametov, A. A., Gabibov, A. G., Shtilman, M. I., Kostoff, R., Carvalho, F., Vinceti, M., Spandidos, D. A., & Tsatsakis, A. (2020). Towards effective COVID-19 vaccines: Updates, perspectives and challenges (Review). *International Journal of Molecular Medicine*, *46*(1), 3–16. https://doi.org/10.3892/ijmm.2020.4596

Chan, J. F. W., Chan, K.-H., Kao, R. Y. T., To, K. K. W., Zheng, B.-J., Li, C. P. Y., Li, P. T. W., Dai, J., Mok, F. K. Y., Chen, H., Hayden, F. G., & Yuen, K.-Y. (2013). Broad-spectrum antivirals for the emerging Middle East respiratory syndrome coronavirus. *The Journal of Infection*, *67*(6), 606–616. https://doi.org/10.1016/j.jinf.2013.09.029

Chaube, U., Chhatbar, D., & Bhatt, H. (2016). 3D-QSAR, molecular dynamics simulations and molecular docking studies of benzoxazepine moiety as mTOR inhibitor for the treatment of lung cancer. *Bioorganic & Medicinal Chemistry Letters*, *26*(3), 864–874. https://doi.org/10.1016/j.bmcl.2015.12.075

Chen, K. C., Chen, H. Y., & Chen, C. Y. C. (2014). Potential protein phosphatase 2A agents from traditional Chinese medicine against cancer. *Evidence-Based Complementary and Alternative Medicine*, *2014*, 436–863.

Chen, Y. C. (2015). *Beware of docking*!. *Trends in Pharmacological Sciences*, *36*(2), 78–95. https://doi.org/10.1016/j.tips.2014.12.001

Chenafa, H., Mesli, F., Daoud, I., Achiri, R., Ghalem, S., & Neghra, A. (2021). In silico design of enzyme α-amylase and α-glucosidase inhibitors using molecular docking, molecular dynamic, conceptual DFT investigation and pharmacophore modelling. *Journal of Biomolecular Structure and Dynamics*, *39*, 1–22.

Choudhary, M. I., Shaikh, M., Tul-Wahab, A., & Ur-Rahman, A. (2020). In silico identification of potential inhibitors of key SARS-CoV-2 3CL hydrolase (Mpro) via molecular docking, MMGBSA predictive binding energy calculations, and molecular dynamics simulation. *PLOS One*, *15*(7), e0235030. https://doi.org/10.1371/journal.pone.0235030

Clément, G., & Slenzka, K. (2006). *Fundamentals of space biology: Research on cells, animals, and plants in space*. Springer.

Daina, A., Michielin, O., & Zoete, V. (2017). SwissADME: A free web tool to evaluate pharmacokinetics, drug-likeness and medicinal chemistry friendliness of small molecules. *Scientific Reports*, *7*, 42717. https://doi.org/10.1038/srep42717

Dal Ben, D., Buccioni, M., Lambertucci, C., Thomas, A., & Volpini, R. (2013). Simulation and comparative analysis of binding modes of nucleoside and non-nucleoside agonists at the A2B adenosine receptor. *In Silico Pharmacology*, *1*(1), 24. https://doi.org/10.1186/2193-9616-1-24

Daoud, I., Melkemi, N., Salah, T., & Ghalem, S. (2018). Combined QSAR, molecular docking and molecular dynamics study on new Acetylcholinesterase and Butyrylcholinesterase inhibitors. *Computational Biology and Chemistry*, *74*, 304–326. https://doi.org/10.1016/j.compbiolchem.2018.03.021

de Wilde, A. H., Jochmans, D., Posthuma, C. C., Zevenhoven-Dobbe, J. C., van Nieuwkoop, S., Bestebroer, T. M., van den Hoogen, B. G., Neyts, J., & Snijder, E. J. (2014). Screening of an FDA-approved compound library identifies four small-molecule inhibitors of middle east respiratory syndrome coronavirus replication in cell culture. *Antimicrobial Agents and Chemotherapy*, *58*(8), 4875–4884. https://doi.org/10.1128/AAC.03011-14

Delaney, J. S. (2005). Predicting aqueous solubility from structure. *Drug Discovery Today*, *10*(4), 289–295. https://doi.org/10.1016/S1359-6446(04)03365-3

Didierjean, C., & Tête-Favier, F. (2016). Introduction to protein science. In *Architecture, function and genomics* (3rd ed., 466p, A. M. Lesk, Eds.). Oxford University Press. ISBN 9780198716846.

Dixon, S. L., Smondyrev, A. M., Knoll, E. H., Rao, S. N., Shaw, D. E., & Friesner, R. A. (2006). PHASE: A new engine for pharmacophore perception, 3D QSAR model development, and 3D database screening: 1. Methodology and preliminary results. *Journal of Computer-Aided Molecular Design*, *20*(10–11), 647–671. https://doi.org/10.1007/s10822-006-9087-6

Dyall, J., Coleman, C. M., Hart, B. J., Venkataraman, T., Holbrook, M. R., Kindrachuk, J., Johnson, R. F., Olinger, G. G., Jahrling, P. B., Laidlaw, M., Johansen, L. M., Lear-Rooney, C. M., Glass, P. J., Hensley, L. E., & Frieman, M. B. (2014). Repurposing of clinically developed drugs for treatment of Middle East respiratory syndrome coronavirus infection. *Antimicrobial Agents and Chemotherapy*, *58*(8), 4885–4893. https://doi.org/10.1128/AAC.03036-14

Ekins, S., Ecker, G. F., Chiba, P., & Swaan, P. W. (2007). Future directions for drug transporter modelling. *Xenobiotica; The Fate of Foreign Compounds in Biological Systems*, *37*(10–11), 1152–1170. https://doi.org/10.1080/00498250701646341

Fagerholm, U. (2007). Prediction of human pharmacokinetics-gastrointestinal absorption. *The Journal of Pharmacy and Pharmacology*, *59*(7), 905–916. https://doi.org/10.1211/jpp.59.7.0001

Furuta, Y., Takahashi, K., Kuno-Maekawa, M., Sangawa, H., Uehara, S., Kozaki, K., Nomura, N., Egawa, H., & Shiraki, K. (2005). Mechanism of action of T-705 against influenza virus. *Antimicrobial Agents and Chemotherapy*, *49*(3), 981–986. https://doi.org/10.1128/AAC.49.3.981-986.2005

Gao, J., Zhenxue, T., & Yang, X. (2020). Breakthrough: Chloroquine phosphate has shown apparent efficacy in treatment of COVID-19 associated pneumonia in clinical studies. *BioScience Trends*, *14*(1), 72-73. https://doi.org/10.5582/bst.2020.01047

Gautret, P., Lagier, J. C., Parola, P., Hoang, V. T., Meddeb, L., Mailhe, M., Doudier, B., Courjon, J., Giordanengo, V., Vieira, V. E., Tissot Dupont, H., Honoré, S., Colson, P., Chabrière, E., La Scola, B., Rolain, J. M., Brouqui, P., & Raoult, D. (2020). Hydroxychloroquine and azithromycin as a treatment of COVID-19: Results of an open-label non-randomized clinical trial. *International Journal of Antimicrobial Agents*, *56*(1), 105949. https://doi.org/10.1016/j.ijantimicag.2020.105949

Guex, N., Peitsch, M. C., & Schwede, T. (2009). Automated comparative protein structure modeling with SWISS-MODEL and Swiss-PdbViewer: A historical perspective. *Electrophoresis*, *30*(S1), S162–S173. https://doi.org/10.1002/elps.200900140

Halgren, T. A. (1996). Merck molecular force field. I. Basis, form, scope, parameterization, and performance of MMFF94. *Journal of Computational Chemistry*, *17*(5–6), 490–519. [Database] https://doi.org/10.1002/(SICI)1096-987X(199604)17:5/6<490::AID-JCC1>3.0.CO;2-P

Halgren, T. A. (1999). MMFF VII. Characterization of MMFF94, MMFF94s, and other widely available force fields for conformational energies and for intermolecular-interaction energies and geometries. *Journal of Computational Chemistry*, *20*(7), 730–748. https://doi.org/10.1002/(SICI)1096-987X(199905)20:7<730::AID-JCC8>3.0.CO;2-T

Hernández-Rodríguez, M., Correa-Basurto, J., Gutiérrez, A., Vitorica, J., & Rosales-Hernández, M. C. (2016). Asp32 and Asp228 determine the selective inhibition of BACE1 as shown by docking and molecular

dynamics simulations. *European Journal of Medicinal Chemistry*, *124*, 1142–1154. https://doi.org/10.1016/j.ejmech.2016.08.028

Hevener, K. E., Zhao, W., Ball, D. M., Babaoglu, K., Qi, J., White, S. W., & Lee, R. E. (2009). Validation of molecular docking programs for virtual screening against dihydropteroate synthase. *Journal of Chemical Information and Modeling*, *49*(2), 444–460. https://doi.org/10.1021/ci800293n

Hou, T. J., Li, Y. Y., & Zhang, W. (2008). Recent developments of in silico predictions of intestinal absorption and oral bioavailability. *Combinatorial Chemistry & High Throughput Screening, 12*(5), 497-506. https://doi.org/10.2174/138620709788489082

Hou, T., Wang, J., Zhang, W., Wang, W., & Xu, X. (2006). Recent advances in computational prediction of drug absorption and permeability in drug discovery. *Current Medicinal Chemistry*, *13*(22), 2653–2667. https://doi.org/10.2174/092986706778201558

Huang, H. J., Lee, C. C., & Chen, C. Y. C. (2014). Lead discovery for Alzheimer's disease related target protein RbAp48 from traditional Chinese medicine. *BioMed Research International*, *2014*, 764946. https://doi.org/10.1155/2014/764946

Hung, T. C., Lee, W. Y., Chen, K. B., Chan, Y. C., Lee, C. C., & Chen, C. Y. C. (2014). In silico investigation of traditional Chinese medicine compounds to inhibit human histone deacetylase 2 for patients with Alzheimer's disease. *BioMed Research International*, *2014*, 769867–769867. https://doi.org/10.1155/2014/769867

HyperChem *v8*. (2009). *Molecular modelling system*. Hypercube Inc.

Imberty, A., Hardman, K. D., Carver, J. P., & Perez, S. (1991). Molecular modelling of protein-carbohydrate interactions. Docking of monosaccharides in the binding site of concanavalin A. *Glycobiology*, *1*(6), 631–642. https://doi.org/10.1093/glycob/1.6.631

Jaworski, J. S., Bankiewicz, B., Krygowski, T. M., Palusiak, M., Stasyuk, O. A., & Szatylowicz, H. (2016). Interactions of polar hydrogen bond donor solvents with ions: A theoretical study. *Structural Chemistry*, *27*(4), 1279–1289. https://doi.org/10.1007/s11224-016-0769-y

Johnson, S. R., & Zheng, W. F. (2006). Recent progress in the computational prediction of aqueous solubility and absorption. *The AAPS Journal*, *8*(1), E27–40. https://doi.org/10.1208/aapsj080104

Jolivette, L. J., & Ekins, S. (2007). Methods for predicting human drug metabolism. *Advances in Clinical Chemistry*, *43*, 131–176. https://doi.org/10.1016/s0065-2423(06)43005-5

Jones, I., & Roy, P. (2021). Sputnik V COVID-19 vaccine candidate appears safe and effective. *Lancet (London, England)*, *397*(10275), 642–643. https://doi.org/10.1016/S0140-6736(21)00191-4

Keyaerts, E., Vijgen, L., Maes, P., Neyts, J., & Van Ranst, M. (2004). In vitro inhibition of severe acute respiratory syndrome coronavirus by Chloroquine. *Biochemical and Biophysical Research Communications*, *323*(1), 264–268. https://doi.org/10.1016/j.bbrc.2004.08.085

Kiefer, F., Arnold, K., Künzli, M., Bordoli, L., & Schwede, T. (2009). The SWISS-MODEL Repository and associated resources. *Nucleic Acids Research*, *37*(Issue suppl_1), D387–D392. https://doi.org/10.1093/nar/gkn750

Klebe, G. (2006). Virtual ligand screening: Strategies, perspectives and limitations. *Drug Discovery Today*, *11*(13–14), 580–594. https://doi.org/10.1016/j.drudis.2006.05.012

Kleywegt, G. J., & Jones, T. A. (1997). [11] Model building and refinement practice. *Methods in Enzymology*, *277*, 208–230.

Lau, S. K. P., Woo, P. C. Y., Li, K. S. M., Huang, Y., Tsoi, H.-W., Wong, B. H. L., Wong, S. S. Y., Leung, S.-Y., Chan, K.-H., & Yuen, K.-Y. (2005). Severe acute respiratory syndrome coronavirus-like virus in Chinese horseshoe bats. *Proceedings of the National Academy of Sciences of the United States of America*, *102*(39), 14040–14045. https://doi.org/10.1073/pnas.0506735102

Le, T., Andreadakis, Z., Kumar, A., Gómez Román, R., Tollefsen, S., Saville, M., & Mayhew, S. (2020). The COVID-19 vaccine development landscape. *Nature Reviews. Drug Discovery*, *19*(5), 305–306. https://doi.org/10.1038/d41573-020-00073-5

Lee, C. Y.-P., Lin, R. T. P., Renia, L., & Ng, L. F. P. (2020). Serological approaches for COVID-19: Epidemiologic perspective on surveillance and control. *Frontiers in Immunology*, *11*, 879. https://doi.org/10.3389/fimmu.2020.00879

Lee, J. S., & Shin, E.-C. (2020). The type I interferon response in COVID-19: Implications for treatment. *Nature Reviews Immunology*, *20*(10), 585–586. https://doi.org/10.1038/s41577-020-00429-3

Liu, X., Ouyang, S., Yu, B., Liu, Y., Huang, K., Gong, J., Zheng, S., Li, Z., Li, H., & Jiang, H. (2010). PharmMapper server: A web server for potential drug target identification using pharmacophore mapping approach. *Nucleic Acids Research*, *38*(Web Server issue), W609–W614. https://doi.org/10.1093/nar/gkq300

Livingston, E. H., Malani, P. N., & Creech, C. B. (2021). The Johnson & Johnson vaccine for COVID-19. *JAMA*, *325*(15), 1575–1575. https://doi.org/10.1001/jama.2021.2927

Luiz, C. S., Pinheiro, L., M Feitosa, L., O Gandi, M., F Silveira, F., & Boechat, N. (2019). The development of novel compounds against malaria: Quinolines, triazolpyridines, pyrazolopyridines and pyrazolopyrimidines. *Molecules*, *24*(22), 4095. https://doi.org/10.3390/molecules24224095

Mahase, E. (2020). Covid-19: Moderna vaccine is nearly 95% effective, trial involving high risk and elderly people shows. *BMJ: British Medical Journal, 371*, 4347. https://doi.org/10.1136/bmj.m4471.

Mani, D., Wadhwani, A., & Krishnamurthy, P. T. (2019). Drug repurposing in antiviral research: A current scenario. *Journal of Young Pharmacists*, *11*(2), 117–121. https://doi.org/10.5530/jyp.2019.11.26

Marechal, Y. (2007). *The hydrogen bond and the water molecule: The physics and chemistry of water, aqueous, and bio-media*. Elsevier.

McChesney, E. W. (1983). Animal toxicity and pharmacokinetics of hydroxychloroquine sulfate. *The American Journal of Medicine*, *75*(1A), 11–18. https://doi.org/10.1016/0002-9343(83)91265-2

Mesli, F., Daoud, I., & Ghalem, S. (2019). Antidiabetic activity of Nigella Sativa (BLACK SEED)-by molecular modeling elucidation, molecular dynamic, and conceptual DFT investigation. *Pharmacophore*, *10*(5), 57–66.

Mesli, F., Ghalem, M., Daoud, I., & Ghalem, S. (2021). Potential inhibitors of angiotensin converting enzyme 2 receptor of COVID-19 by Corchorus olitorius Linn using docking, molecular dynamics, conceptual DFT investigation and pharmacophore mapping. *Journal of Biomolecular Structure and Dynamics*, *39*, 1–13.

Molecular Operating Environment (Moe). (2019)., 2013.08; Chemical Computing Group Inc., 1010 Sherbooke St. West, Suite #910, Montreal, QC, H3a 2r7.

Müller, L., Andrée, M., Moskorz, W., Drexler, I., Walotka, L., Grothmann, R., Ptok, J., Hillebrandt, J., Ritchie, A., Rabl, D. and Ostermann, P.N., Robitzsch, R., Hauka, S., Walker, A., Menne, C., Grutza, R., Timm, J., Adams, O., Schaal, H. (2021). Age-dependent immune response to the Biontech/Pfizer BNT162b2 COVID-19 vaccination. *Clin Infect Dis*., ciab381. https://doi.org/10.1093/cid/ciab381. Epub ahead of print. PMID: 33906236; PMCID: PMC8135422.

Nadia, B., Mesli, F., Zahra, B. F., Merad-Boussalah, N., Radja, A., Muselli, A., Djabou, N., & Dib, M. E. A. (2020). Chemical composition variability and vascular endothelial growth factor receptors inhibitory activity of Inulaviscosa essential oils from Algeria. *Journal of Biomolecular Structure and Dynamics*, *39*, 1–19.

Narkhede, R. R., Cheke, R. S., Ambhore, J. P., & Shinde, S. D. (2020). The molecular docking study of potential drug candidates showing anti-COVID-19 activity by exploring of therapeutic targets of SARS-CoV-2. *Eurasian Journal of Medicine and Oncology*, *4*(3), 185–195.

National Institutes of Health (NIH). (2020). 17 March "New coronavirus stable for hours on surfaces". Retrieved 24 March 2020.

Norinder, U., & Bergstrom, C. A. S. (2006). Prediction of ADMET properties. *ChemMedChem*, *1*(9), 920–937. https://doi.org/10.1002/cmdc.200600155

Norinder, U., & Haeberlein, M. (2002). Computational approaches to the prediction of the blood-brain distribution. *Advanced Drug Delivery Reviews*, *54*(3), 291–313. https://doi.org/10.1016/S0169-409X(02)00005-4

Omrani, A. S., Saad, M. M., Baig, K., Bahloul, A., Abdul-Matin, M., Alaidaroos, A. Y., Almakhlafi, G. A., Albarrak, M. M., Memish, Z. A., & Albarrak, A. M. (2014). Ribavirin and interferon alfa-2a for severe Middle East respiratory syndrome coronavirus infection: A retrospective cohort study. *The Lancet Infectious Diseases*, *14*(11), 1090–1095. https://doi.org/10.1016/S1473-3099(14)70920-X

Palacios, R., Patiño, E. G., de Oliveira Piorelli, R., Conde, M. T. R. P., Batista, A. P., Zeng, G., Xin, Q., Kallas, E. G., Flores, J., Ockenhouse,

C. F., & Gast, C. (2020). Double-blind, randomized, placebo-controlled phase iii clinical trial to evaluate the efficacy and safety of treating healthcare professionals with the adsorbed COVID-19 (inactivated) vaccine manufactured by Sinovac - PROFISCOV: A structured summary of a study protocol for a randomised controlled trial. *Trials*, *21*(1), 853–853. https://doi.org/10.1186/s13063-020-04775-4

Panisheva, E. K., Mikerova, N. I., Nikolaeva, I. S., Fomina, A. N., Cherkasova, A. A., Golovanova, E. A., & Krylova, L. Y. (1988). Synthesis and antiviral activity of 5-oxyindole derivatives. *Pharmaceutical Chemistry Journal*, *22*, 901–904.*1*

Parr, R. G. & Yang, W. (1980). *Density functional theory of atoms and molecules* (Vol. 1, 989p). Oxford University Press.

Reusken, C. B. E. M., Haagmans, B. L., Müller, M. A., Gutierrez, C., Godeke, G.-J., Meyer, B., Muth, D., Raj, V. S., Smits-De Vries, L., Corman, V. M., Drexler, J.-F., Smits, S. L., El Tahir, Y. E., De Sousa, R., van Beek, J., Nowotny, N., van Maanen, K., Hidalgo-Hermoso, E., Bosch, B.-J., … Koopmans, M. P. G. (2013). Middle East respiratory syndrome coronavirus neutralising serum antibodies in dromedary camels: A comparative serological study. *The Lancet Infectious Diseases*, *13*(10), 859–866. https://doi.org/10.1016/S1473-3099(13)70164-6

Robertson, C. C., Wright, J. S., Carrington, E. J., Perutz, R. N., Hunter, C. A., & Brammer, L. (2017). Hydrogen bonding vs. halogen bonding: The solvent decides. *Chemical Science*, *8*(8), 5392–5398. https://doi.org/10.1039/c7sc01801k

Rosales-Mendoza, S., MáRquez-Escobar, V. A., & GonzáLez-Ortega, O. (2020). What does plant-based vaccine technology offer to the fight against COVID-19? *Vaccines*, *8*, 183. https://doi.org/10.3390/vaccines8020183

Ryzhikov, A. B., Ryzhikov, E. A., Bogryantseva, M. P., Usova, S. V., Danilenko, E. D., Nechaeva, E. A., Pyankov, O. V., Pyankova, O. G., Gudymo, A. S., Bodnev, S. A., Onkhonova, G. S., Sleptsova, E. S., Kuzubov, V. I., Ryndyuk, N. N., Ginko, Z. I., Petrov, V. N., Moiseeva, A. A., Torzhkova, P. Y., Pyankov, S. A., … Maksyutov, R. A. (2021). A single blind, placebo-controlled randomized study of the safety, reactogenicity and immunogenicity of the "EpiVacCorona" Vaccine for the prevention of COVID-19, in volunteers aged 18–60 years (phase I-II). *Russian Journal of Infection and Immunity*, *11*(2), 283–296. https://doi.org/10.15789/2220-7619-ASB-1699

Sakurai, Y., Kolokoltsov, A. A., Chen, C.-C., Tidwell, M. W., Bauta, W. E., Klugbauer, N., Grimm, C., Wahl-Schott, C., Biel, M., & Davey, R. A. (2015). Ebola virus. Two-pore channels control Ebola virus host cell entry and are drug targets for disease treatment. *Science (New York, NY)*, *347*(6225), 995–998. https://doi.org/10.1126/science.1258758

Silva, T. B., Bernardino, A. M., Maria de Lourdes, G. F., Rogerio, K. R., Carvalho, L. J., Boechat, N., & Pinheiro, L. C. (2016). Design, synthesis and anti-P. falciparum activity of pyrazolopyridine-sulfonamide derivatives. *Bioorganic & Medicinal Chemistry*, *24*(18), 4492–4498. https://doi.org/10.1016/j.bmc.2016.07.049

Stewart, J. J. P. (2007). Optimization of parameters for semiempirical methods V: Modification of NDDO approximations and application to 70 elements. *Journal of Molecular Modeling*, *13*(12), 1173–1213. https://doi.org/10.1007/s00894-007-0233-4

Sturgeon, J. B., & Laird, B. B. (2000). Symplectic algorithm for constant-pressure molecular-dynamics using a Nose-Poincare thermostat. *Journal of Chemical Physics*, *112*(8), 3474–3482. https://doi.org/10.1063/1.480502

Thomsen, R., & Christensen, M. H. (2006). MolDock: A new technique for high-accuracy molecular docking. *Journal of Medicinal Chemistry*, *49*(11), 3315–3321. https://doi.org/10.1021/jm051197e

Van De Waterbeemd, H., & Gifford, E. (2003). ADMET in silico modelling: Towards prediction paradise? *Nature Reviews. Drug Discovery*, *2*(3), 192–204. https://doi.org/10.1038/nrd1032

Varadwaj, P. R., Varadwaj, A., Marques, H. M., & Yamashita, K. (2019). Significance of hydrogen bonding and other noncovalent interactions in determining octahedral tilting in the CH3NH3PbI3 hybrid organic-inorganic halide perovskite solar cell semiconductor. *Scientific Reports*, *9*(1), 50–29. https://doi.org/10.1038/s41598-018-36218-1

Vincent, M. J., Bergeron, E., Benjannet, S., Erickson, B. R., Rollin, P. E., Ksiazek, T. G., Seidah, N. G., & Nichol, S. T. (2005). Chloroquine is a potent inhibitor of SARS coronavirus infection and spread. *Virology Journal*, *2*, 69. https://doi.org/10.1186/1743-422X-2-69

Wang, X., Pan, C., Gong, J., Liu, X., & Li, H. (2016). Enhancing the enrichment of pharmacophore-based target prediction for the polypharmacological profiles of drugs. *Journal of Chemical Information and Modeling*, *56*(6), 1175–1183. https://doi.org/10.1021/acs.jcim.5b00690

Wang, X., Shen, Y., Wang, S., Li, S., Zhang, W., Liu, X., Lai, L., Pei, J., & Li, H. (2017). PharmMapper 2017 update: A web server for potential drug target identification with a comprehensive target pharmacophore database. *Nucleic Acids Research*, *45*(W1), W356–W360. https://doi.org/10.1093/nar/gkx374

Wang, Y., Zhang, D., Du, G., Du, R., Zhao, J., Jin, Y., Fu, S., Gao, L., Cheng, Z., Lu, Q., Hu, Y., Luo, G., Wang, K., Lu, Y., Li, H., Wang, S., Ruan, S., Yang, C., Mei, C., … Wang, C. (2020). Remdesivir in adults with severe COVID-19: A randomised, double-blind, placebocontrolled, multicentre trial. *The Lancet*, *395*(10236), 1569–1578. https://doi.org/10.1016/S0140-6736(20)31022-9

Warren, T. K., Jordan, R., Lo, M. K., Ray, A. S., Mackman, R. L., Soloveva, V., Siegel, D., Perron, M., Bannister, R., Hui, H. C., Larson, N., Strickley, R., Wells, J., Stuthman, K. S., Van Tongeren, S. A., Garza, N. L., Donnelly, G., Shurtleff, A. C., Retterer, C. J., … Bavari, S. (2016). Therapeutic efficacy of the small molecule GS-5734 against Ebola virus in rhesus monkeys. *Nature*, *531*(7594), 381–385. https://doi.org/10.1038/nature17180

Wise, J. (2021). Covid-19: European countries suspend use of Oxford-AstraZeneca vaccine after reports of blood clots. *BMJ (Clinical Research ed.)*, *372*, n699. https://doi.org/10.1136/bmj.n699

Witkowski, J. T., Robins, R. K., Sidwell, R. W., & Simon, L. N. (1972). Design, synthesis, and broad spectrum antiviral activity of 1-D-ribofuranosyl-1,2,4-triazole-3-carboxamide and related nucleosides. *Journal of Medicinal Chemistry*, *15*(11), 1150–1154. https://doi.org/10.1021/jm00281a014

Wu, C., Liu, Y., Yang, Y., Zhang, P., Zhong, W., Wang, Y., Wang, Q., Xu, Y., Li, M., Li, X., Zheng, M., Chen, L., & Li, H. (2020). Analysis of therapeutic targets for SARS-CoV-2 and discovery of potential drugs by computational methods. *Acta Pharmaceutica Sinica B*, *10*(5), 766–788. https://doi.org/10.1016/j.apsb.2020.02.008

Xie, N. Z., Du, Q. S., Li, J. X., & Huang, R. B. (2015). Exploring strong interactions in proteins with quantum chemistry and examples of their applications in drug design. *PLoS One*, *10*(9), e0137113. https://doi.org/10.1371/journal.pone.0137113

Xu, M., Zhang, B., Wang, Q., Yuan, Y., Sun, L., & Huang, Z. (2018). Theoretical study on the hydrogen bonding interactions in paracetamol-water complexes. *Journal of the Chilean Chemical Society*, *63*(1), 3788–3794. https://doi.org/10.4067/s0717-97072018000103788

Zaretzki, J., Bergeron, C., Huang, T. W., Rydberg, P., Swamidass, S. J., & Breneman, C. M. (2013). RS-WebPredictor: A server for predicting CYP-mediated sites of metabolism on drug-like molecules. *Bioinformatics (Oxford, England)*, *29*(4), 497–498. https://doi.org/10.1093/bioinformatics/bts705

Zumla, A., Chan, J. F., Azhar, E. I., Hui, D. S., & Yuen, K. Y. (2016). Coronaviruses - drug discovery and therapeutic options. *Nature Reviews. Drug Discovery*, *15*(5), 327–347. https://doi.org/10.1038/nrd.2015.37